

The Preserve: Lehigh Library Digital Collections

Composite Sandwich Panels

Citation

Truxel, Andrew. *Composite Sandwich Panels*. 2009, https://preserve.lehigh.edu/lehigh-scholarship/graduate-publications-theses-dissertations/theses-dissertations/composite-0.

Find more at https://preserve.lehigh.edu/

This document is brought to you for free and open access by Lehigh Preserve. It has been accepted for inclusion by an authorized administrator of Lehigh Preserve. For more information, please contact preserve@lehigh.edu.

Composite Sandwich Panels

by

Andrew Truxel

Presented to the Graduate and Research Committee

of Lehigh University

in Candidacy for the Degree of

Doctor of Philosophy

In

Mechanical Engineering and Mechanics

Lehigh University

Bethlehem, PA

September 2009

Certificate of Approval

Approved and recommended for acceptance as a dissertation in partial fulfillment of the requirements for the degree of Doctor of Philosophy.

_____
Date

_____
Dissertation Director

_____
Accepted Date

Committee Members:

_____
Dr. Joachim L. Grenestedt, Dissertation Advisor/Committee Chairman
Professor
Department of Mechanical Engineering and Mechanics

_____
Dr. Terry J. Delph
Professor
Department of Mechanical Engineering and Mechanics

_____
Dr. James M. Ricles
Professor, Director, Real-Time Multi-directional Earthquake Simulation Facility
Department of Civil and Environmental Engineering

_____
Dr. Herman F. Nied
Professor
Department of Mechanical Engineering and Mechanics

Acknowledgements

I wish to express gratitude to the following:

-Professor Joachim Grenestedt for his patience, teaching and support as advisor to the research contained in this dissertation. His ‘can-do’ attitude, inquisitive mind, and get your ’hands dirty’ mentality, made for an enjoyable learning environment.

-Dr. Terry Delph, Dr. James Ricles, and Dr Herman Nied of my amazing PhD committee who gave me guidance and direction throughout my quest to obtain a terminal degree.

-Research Engineer Bill Maroun who has taken time every day to explain to me the fundamentals of engineering, manufacturing and ten thousand and one uses for scotch brite.

-Fellow Lehigh students Jun Cao, Matt Kampner, Jack Reany, Scott Shirey, and Jian Lv who have often lended a hand or two with research and moving molds.

-My friends and family who always encouraged and supported me especially when I needed it most.

Table of Contents

Dissertation
Abstract……..…….……1

Chapter 1
Dissertation
Introduction……..…….....4

Chapter 2
Doubly curved composite sandwich panels……8

Chapter 3
Large Steel/Composite Hybrid Beam. Part I: Design and Manufacture…….....51

Chapter 4
FRP sandwich tensile tests with embedded strain gages……..……....87

Chapter 5
Summary, Conclusions, and recommendations for future work……..……...107

References…….....112

Appendix A…….117

Dissertation Abstract

The work leading up to this thesis dealt in particular with the fabrication of composite sandwich panels for use in marine structures. Methods for making complex sandwich panels and the forming of the foam cores for complex panels were experimentally studied.

There is scarce information on hydrostatically loaded doubly curved composite sandwich panels. In particular their fabrication and the affect curvature has on their performance.

Doubly curved composite sandwich panels loaded by evenly distributed pressure were designed, analyzed, manufactured and tested. Quick and cost effective methods for making molds for vacuum infused doubly curved sandwich panels were studied and implemented. Several different manufacturing techniques for making doubly curved panels and doubly curved foam cores were investigated. Tests were performed using a hydrostatic water tank.

Doubly curved composite sandwich panels with a thin light foam core and stiff skins in comparison to a flat panel is much more affected by an increase in curvature than a panel with a thick, denser foam core and less stiff skins. A time and cost effective method for fabricating a doubly curved panel is to first CNC route the shape from a high density foam, then CNC route the foam core flat and thermoform it to shape in the

mold, then cover the mold with either epoxy or vacuum bag and layup the panel and vacuum infuse. For the panel to be watertight care must be taken during vacuum infusion so there are no air leaks. The predicted results showed good correlation to experimental results, within 1.2% difference for deflection.

Previous work has been done on a hybrid hull concept for a five-sided ship hull cross section, having a steel frame designed to take the global bending loads, and bonded fiberglass sandwich panels designed to take shear and water pressure loads. Wave induced loads were calculated using the American Bureau of Shipping (ABS) guidelines for a 142m (water line length) destroyer class ship, and applied to a 1:35 scale model. This model had a constant cross section and it was tested in a six-point bending setup. The model exhibited excellent global ductility, something that would not be expected from an all-composite structure. The beam was tested to 36% above the design load, which resulted in yielding within the steel truss and permanent global deformation but otherwise no damage. In particular there were no failures within the composite panels or bonded joints. This work has been extended to build a much larger 1:8 scale hybrid hull and study its fatigue performance.

Both conventional (flat) and corrugated skin sandwich panels with the size 1.34 m x 1.59 m were designed and manufactured for a large hybrid ship hull specimen. This specimen had the geometric shape of an existing bridge girder for a magnetically levitated train, which was retrofitted and tested as a 1:8 scale model of a destroyer class ship. A three point bending fatigue testing fixture was developed, and the specimen

was fatigue tested for 325,000 cycles. Cracks were found in the steel of the specimen, but almost no damage occurred in the bonded joints or the composite panels. The flat sandwich panels were very much lighter than the steel they replaced, and the corrugated panels were even 15% lighter than the flat panels.

A steel/composite hybrid hull for an 8.75m, high-speed boat is currently being manufactured. This craft will serve as an instrumented slamming load test facility. A method has been developed to measure strains on the outer skins without having strain gages attached to the outside; gages on the outside could be damaged during testing. The strain gages were placed between the outer skin and the foam core of the sandwich panels. The manufacturing process of embedding strain gages inside composite sandwich panels is discussed. Two different test panels were fabricated, one to test the method of embedding strain gages inside sandwich panels and the other to compare the readings of the strain gages inside the panel verses outside. The difference between the embedded strain gages and strain gages mounted to the outside of the specimen were within 3%.

Chapter 1

Dissertation Introduction

Since the beginning of time there has been a trend towards making stronger, more lightweight and more cost effective structures. These structures can be found almost everywhere, including in aerospace, naval, automotive and public transportation vehicles, bridges and other civil infrastructure, sporting equipment, etc. Composite sandwich structures are particularly well suited for aerospace and marine vehicles because of high strength and stiffness to weight ratios, high corrosion and fatigue resistances, and the ability to be manufactured into complex shapes. There is little published research on quick and cheap mold manufacturing to make these sandwich structures into complex shapes. There is also scarce literature on doubly curved sandwich panels tested under hydrostatic water pressure or what effect curvature has on panels under this loading. But before the doubly curved sandwich panels can be tested under hydrostatic pressure they need to be attached to a steel fixture that could be similar to the composite sandwich/steel hybrid hull concept. The hybrid hull concept has only been tested under simplified small scale conditions. There is no previous data on how the hybrid hull concept performs in fatigue, in a larger scale test, or even if the concept will float. Currently there have been no hybrid hull crafts manufactured and sea tested. If a hybrid hull was manufactured, the behavior of the composite sandwich panels in rough seas would be very useful information. Unfortunately, there are no durable, cost effective means to measure the strains on the outer skins in sea trials. The objectives of this thesis are to try and better understand some of the previously

mentioned issues with composite sandwich panels including the following. Develop a parameter study of the effect of curvature on composite sandwich panels made from various materials and geometries with different boundary conditions. Study cheap and quick manufacture of doubly curved molds and doubly curved panels. The testing of doubly curved sandwich panels under hydrostatic water pressure will be studied with a comparison to numerical models. The manufacture of a larger scale hybrid hull concept to be fatigue tested. Designing and manufacturing the sandwich panels for hybrid hull including corrugated sandwich panels that are lighter then conventional flat panels. Methods for attaching the composite sandwich panels to the steel frame of the hybrid hull will also be investaged. Developing methods of measuring strain on the outside of a sea vessel with a hybrid hull that is tested under harsh sea conditions. Lastly, experimental validation of a method to measure strain on the outside of a sea vessel and the comparison to conventional strain measuring methods.

A typical sandwich panel consists of three layers; two strong and stiff skins attached on either side of a low density core. The strong skins take most of the in-plane and bending loads. Glass fiber reinforced plastic (GFRP) and carbon fiber reinforced plastic (CFRP) are commonly used for the skins. The lightweight core separates the face sheets to increase the bending stiffness of the structure. The core does not contribute much to the bending or in-plane strength but needs to be strong enough to carry most of the transverse shear loads. A composite sandwich panel is analogous to an I-beam in that the skins act like the flanges and the core acts like the web.

When making composite parts with complex geometry a considerable amount of time and money goes into making the molds. Molds used for high production rates are usually made from metal, are heavy, expensive, and time consuming to machine. When vacuum infusing large complex composite sandwich panels, only one side of a mold is needed since the other side is a vacuum bag. To make a large metal mold that would be used only a couple of times for, say, a pleasure boat would be prohibitively expensive. Instead molds are made from other materials such as wood, plastic, foam, fiberglass or a combination of materials. There is no 'best' way to make a mold. Although there are very skilled mold makers that can make molds with very tight tolerances by hand, for this discussion it is assumed that the molds would be CNC machined or routed. Each mold depends upon several things. The area, depth, tolerance, etc. Tooling boards of epoxy or polyurethane are well suited as mold material for shallow parts with relatively high tolerances requirements. Parts with very low tolerance requirements can be made using molds machined from low cost polystyrene foam which are covered with a thin plastic film. Anything in between varies on a case by case basis. For example, in the second chapter of this thesis doubly curved sandwich panels were made. The size was not prohibitive for using a medium density tooling board, which could provide a sufficiently tight tolerance. The panels manufactured in the third chapter were approximately 2m x 1.5m and flat on one side, so a large flat aluminum infusion table was used as the "mold". The cores on the opposite sides of these panels were either chamfered or deeply corrugated and the vacuum bags conformed easily to these complex geometries. The bottom panels for the 8.75m steel/composite hybrid high-speed boat presently being built in the lab were on the order of 2m x 1m. These panels

were rather flat but with a pronounced spray rail at the chine. For this application female molds were made by CNC machining large polystyrene foam blocks, covering the machined surfaces with a tooling paste, and machining the final mold. The result was lightweight but still stiff molds with a thick styrofoam base and a hard approximately 8mm thick layer of the cured tooling paste. The surface was be sealed by a thin coat of epoxy, lightly sanded, and release coated. Very nice panels were vacuum infused directly on these molds. Making these molds and bottom panels has been an important part of the work leading to this thesis. The fourth chapter discusses the strain gages embedded in these bottom panels.

Chapter 2

DOUBLY CURVED COMPOSITE SANDWICH PANELS

Since the beginning of time there has been a trend towards making stronger, more lightweight and more cost effective structures. These structures can be found almost everywhere, ranging from Lockheed Martin's F-35 Joint Strike Fighter, to Lotus's Elite all glass-fiber moncoque chassis, to Marstrom's Tornado glass fiber/epoxy catamaran. Composite sandwich structures are particularly well suited for aerospace and marine vehicles because of high strength and stiffness to weight ratios, high corrosion and fatigue resistances, and the ability to be manufactured into complex shapes.

Many advanced structures have complex curved geometries that complicate accurate design and analysis. There is plenty of literature on doubly curved shells, investigating buckling, vibration, etc., but considerably less on doubly curved panels subjected to hydrostatic pressure. Librescu and Hause [1] did a survey of the developments in the modeling and behavior of advanced sandwich constructions, focusing in particular on post-buckling. Hohe and Librescu [2] investigated a nonlinear theory for doubly curved sandwich shells. Drake et. al. [3] did analytical approximations for a square panel with flat top skin and curved bottom skin loaded with a uniform pressure. Burton and Noor [4] compared nine different 2D modeling approaches for curved shells under thermal loadings. Skvortsoc et al. [5] assessed different models for simply supported beams with single curvature loaded under uniform pressure. O'Sullivan and Slocum [6] studied

alternatives to honeycomb and corrugated core sandwich designs with double curvature. Russo and Zuccarello [7] investigated the failure modes of glass fiber reinforced plastic (GFRP) sandwich panels both experimentally and numerically with non linear Finite Element (FE) models. MacDonald and Chen [8] analytically studied simply supported rectangular sandwich panels with small initial curvature under general loading. Thompson et al. [9] studied flat composite sandwich panels loaded with hydrostatic pressure both experimentally and numerically. Cunningham et. al. [10] studied the effect of curvature, material, fiber orientation, and boundary conditions using a FE model and did experimental free vibration tests on carbon fiber skin / honeycomb core sandwich panels.

Hydrostatic pressure is of particular importance for ship hull panels. Hydrostatically loaded doubly curved panels is the focus of this chapter. Panels were numerically analyzed, manufactured, and then tested under hydrostatic loading.

There have been few studies on inexpensive mold manufacturing methods for complex shaped vacuum infused parts. Kuppusamy [11] studied rapid tool manufacture for several different cases and listed different tool materials for a Resin Infusion between Double Flexible Tooling (RIDFT) process which is similar to Vacuum Assisted Resin Transfer Molding (VARTM). McCaffery et. al. [12] studied low cost mold development for Resin Transfer Molding (RTM) and concluded that the optimal mold should be plastic with wood stiffeners.

Geometry of Experimental Test Panels

The width of sandwich panels on high speed light craft ranging from smaller motorboats to ships well over 50 m in length is typically on the order of 0.5 or 1 m. For the present study, a panel size of 0.6m x 0.6m was chosen for the experimental testing. Apart from being of a relevant size, it also had the benefit of fitting in existing CNC machines including a 5-axis router and an abrasive waterjet cutter. The panels were doubly curved, made in a doubly curved mold, and consisted of an outer skin, a lightweight PVC foam core which was smaller than the panel, an inner skin, plus some additional layers to be explained shortly. A schematic of a panel is shown in Fig. 1. The core was smaller than the panel and tapered off such that the inner and outer skins joined to form a single skin flange at the edge of the panel. This single skin edge would be very thin and weak unless reinforced. Thus some "thickening layers" of coarse fiber architecture were added between the skins at the edge. Further, the area around the tapered part of the foam core was covered with additional "reinforcing layers" to prevent failure; see Fig. 1. The single skin edge is of particular interest for steel / composite ship hulls, where the hull consists of a stainless steel frame to which lightweight sandwich panels are bonded; see for example Cao et al. [13,14], Maroun et al. [15], and Grenestedt [16].

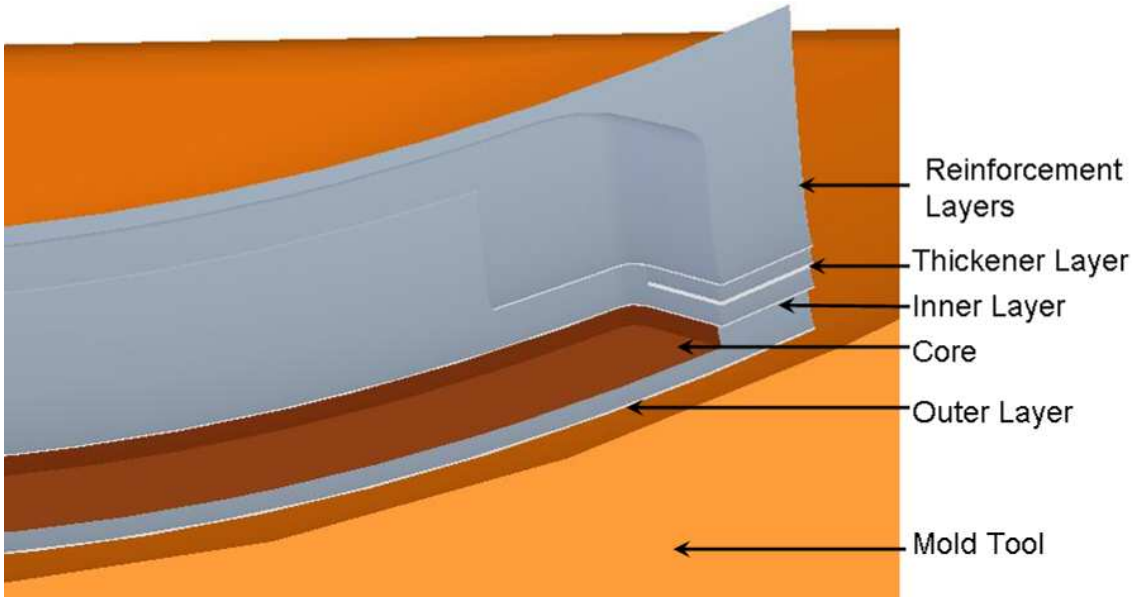


Fig. 1. Panel Geometry.

In order to test the panel under hydrostatic pressure it needs to be attached to a test fixture. After the panels were vacuum infused, they were trimmed and bonded to a steel test fixture interface that was bolted to a hydrostatic pressure tank. The fixture essentially consisted of a welded steel collar ending in a stainless steel "bonding plate" to which the double curvature sandwich panels were bonded, Fig. 2. The fixture mimics the panel attachment to steel bulkheads and longerons on a full-scale hybrid ship that is presently being built at Lehigh University.



Fig. 2. Test fixture.

Finite Element Analysis

Ansys Academic Teaching Advanced 11.0 was used for the modeling and Finite Element (FE) analysis. Due to symmetry only one quarter of the panel was modeled. The shape of the outer skin of the double curved panels was defined by

$$z = \frac{x^2}{2r_a} + \frac{y^2}{2r_b} \qquad (1)$$

where x, y, and z are Cartesian coordinates, and r_a and r_b are parameters related to the radii of curvature of the panel about their respective axes[1]. The edges of the panel were at x=+/-a/2, and y=+/-b/2, where a is the length and b is the width of the panel.

The panel design can be broken up into four parts: inner (facing) skin, foam core, various reinforcement layers along the perimeter of the panel, and the outer (backing) skin. As already mentioned, this panel design shown in Fig. 1, where the foam cores tapers off to a single skin edge is similar to composite panels on some steel/composite hybrid ship hulls [13-16].

The thickness of the single skin flange was designed by limiting the average shear stress τ to 10 MPa, and thus

$$\tau = \frac{Pab}{2(a+b)t_{flange}} \leq 10MPa \quad (2)$$

where τ is the average shear stress, P is the pressure, t_{flange} is the total thickness of the flange (including inner and outer skins, thickener layers, and reinforcement layers), and a and b are the panel width and length, respectively. The fact that the perimeter length increases with curvature was ignored. Rearranging Eq. 2 yields:

$$t_{flange} = \frac{Pab}{2(a+b)\tau} \quad (3)$$

[1] For this study, r_a is always equal to r_b and r_a is used

Sandwich structures can be analyzed using either 2D shell elements, 3D solid elements, or a combination where the sandwich core is modeled with 3D solid elements while the skins are modeled with 2D shell elements. A comparative study between two different modeling approaches was made - using 3D brick elements for the core and 2D shell elements for the skins and using 2D shell elements for the complete sandwich (skins and core). The conclusion was that they produced similar results for the panels under investigation. Both approaches are used subsequently in this chapter - 2D elements only for a larger parameter study, and 3D elements for the core and 2D for the skins for some select panels. The results from the comparative analysis can be seen in Fig. 3; where the x axis label corresponds to different locations where strain was measured and the y axis is the strain value. The data will be discussed in greater detail later.

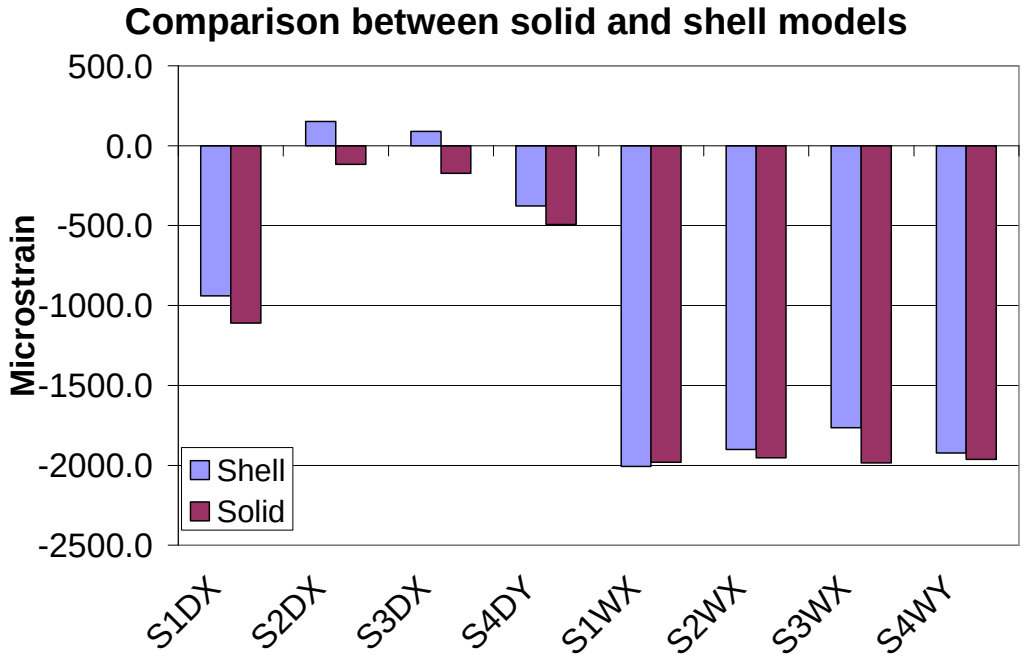


Fig. 3. Solid and Shell results for strain gage locations.

For the solid model (3D core and 2D skins), Solid95 elements were used to model the core and Shell91 elements were used to model the face sheets. Solid95 is a higher order version of the 3D 8-node solid element Solid45. It can tolerate irregular shapes without losing much of its accuracy. Solid95 elements have compatible displacement shapes and are well suited to model curved boundaries, [16].

For the 2D shell model, 8-node, Shell91 elements were used, with the 'sandwich logic' option turned on. The Shell91 elements are defined by layer thicknesses, material direction angles and orthotropic material properties. The total thickness of each element must be less than twice the radius of curvature and when using sandwich logic the core must be at least 5/6 the total thickness. Sandwich logic is specifically designed for sandwich construction with thin face sheets and a thick and relatively compliant core. The core is assumed to carry all of the transverse shear and the face sheets are assumed to carry all (or almost all) of the bending load [17]. The 45 degree taper of the foam core was modeled by modifying the 'real constants' (specifically the lay-up details) of the layered Shell91 elements and the nodes were located on the bottom surface of each element so the taper and flange were in the correct position. Using the sandwich logic option for all the elements that included the foam core meant the 45 degree taper was defined with the thicker half having the sandwich option turned on and the thinner half having the sandwich option turned off (since the thinner half of the tapered foam core would not be at least 5/6 of the total thickness). More information on the elements used can be found in Appendix A.

Parameter study

Numerous numerical simulations were run with varying skin thickness and skin material, core thickness and core material, radii of curvature of the panel, and length-to-width aspect ratios to study their effect on panels with double curvature. For this parameter study, a simplified sandwich model was used with face sheets on either sides of a foam core. The previously mentioned tapered model will be discussed later. The simplified model used 2D shell elements with isotropic material properties. For the (fiberglass) skins, Young's modulus of E=30 GPa and Poisson's ratio of ν=0.3 were assumed. The material properties for the different PVC foam cores are listed in Table 1 (Poisson's ratio ν=0.32 was used for all foam densities).

Table 1. Core Material Properties [19].

Quality		**H80**	**H100**	**H200**	**H250**
Density	kg/m^3	80	100	200	250
Compressive Strength	MPa	1.4	2	5	6
Compressive Modulus	MPa	90	135	240	300
Tensile Strength	MPa	2.5	4	7	9
Tensile Modulus	MPa	95	130	250	320
Shear Strength	MPa	1.15	2	4	5
Shear Modulus	MPa	27	35	85	104
Shear Strain	%	30	40	40	40

The panels were modeled as a sandwich with the nodes located at the midplane and constrained in the z direction at the perimeter. A hydrostatic design pressure of 150 kPa was applied normal to the midplane of the panel. The panels were constrained at their

edges. Symmetry boundary conditions were applied to the planes of symmetry at $x = 0$ and $y = 0$, respectively. In summary, the boundary conditions were u_z=0 at the edge of the panel; u_x=0 and θ_y=θ_z=0 at x=0; and u_y=0 and θ_x=θ_z=0 at y=0. Snapshots of the FE models can be found in Appendix A.

Various simulations were run looping over different variables to study their effect on doubly curved panels. Throughout the study, isotropic material properties, PVC foam cores, and a 150kPa pressure loading were used. The variations of parameters consisted of face sheet stiffness, face sheet thickness, foam core thickness, foam core strength, boundary conditions and length to width aspect ratio. Some of these parameters were studied in detail but for conciseness, the following are mainly discussed; The face sheet stiffnesses were either 30 or 100 GPa to represent GFRP or Carbon Fiber Reinforced Plastic (CFRP). The face sheet thicknesses were either 0.5mm or 2mm. The core thicknesses were either 12.7mm (thin) or 50.8mm (thick). The different foam core types used properties from DIAB Inc's Divinycell H-Grade PVC foam cores of either H80 or H250; table 1. Boundary conditions (BC) of clamped, hinged, or simply supported were used. The length to width aspect ratio varied between 1 and 2.

Reduction in the dimensionality of the model was achieved by using the following dimensionless parameters: a/r_a where a is panel length and r_a is radius of curvature, U/U_{flat}, where U is the max panel deflection in the z direction and U_{flat} is the max panel deflection in the z direction of a flat panel with otherwise identical parameters, t/d

where t is the skin thickness and d is the core thickness, and E_s/E_c where E_s is Young's modulus of the skins and E_c is Young's modulus of the core material.

Fig. 4 shows how the U/U_{flat} varies with curvature for different t/d and E_s/E_c values; the skin thicknesses, t, are held constant while the upper two curves have a 50.8mm thick foam core, the middle two curves have a 25.4mm thick foam core and the lower two curves have a 12.7mm foam core. Each of the three foam core thicknesses have a combination of either H80 foam core with CFRP face sheets or H250 foam core with GFRP face sheets; E_s/E_c of 1080 and 97 respectively. Generally speaking, panels with more curvature (smaller r_a) deflect less than flat panels, the core thickness affects the shape of the curve, and higher E_s/E_c values translate the graph down. For example, the deflection of a panel with a thin light foam core and stiff skins in comparison to a flat panel is much more affected by an increase in curvature than a panel with a thick, denser foam core and less stiff skins. However, it should be noted that for certain configurations curved panels deflect more than a corresponding flat panel, a phenomenon which will be discussed later in greater detail later.

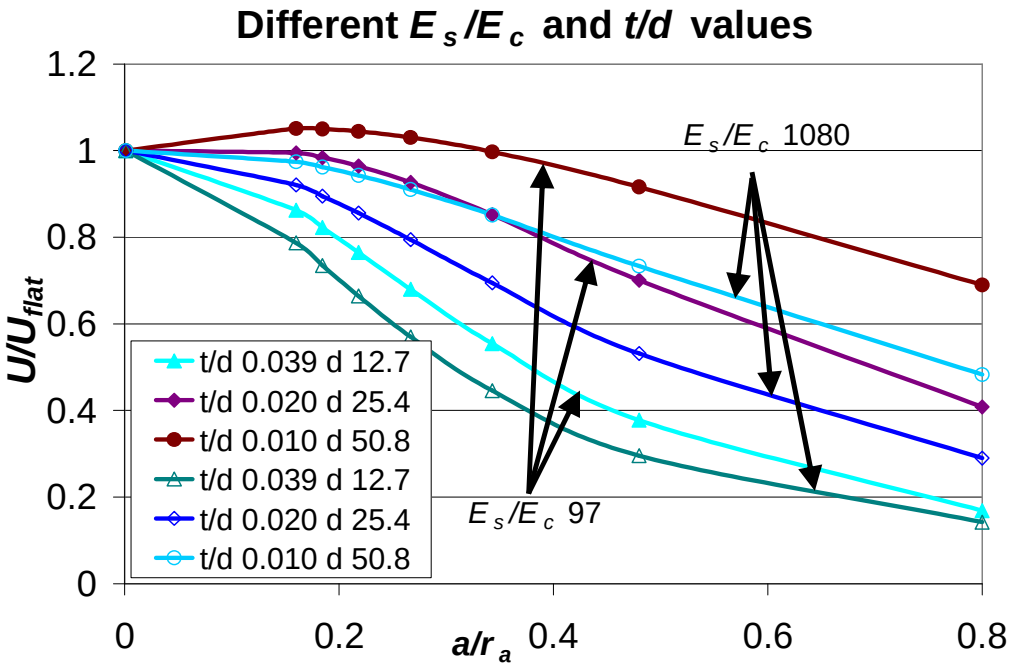


Fig. 4. Comparison between different *Es/Ec* and *t/d* values.

The effect of curvature on panels with different boundary conditions was studied by looking at curved panels with an H80 core, GFRP face sheets (E_s/E_c of 324), and the following boundary conditions. Simply supported, or $u_z=0$ along the edge $x=a/2$, and along the edge $y=b/2$ was the first boundary condition denoted BC1. The boundary conditions were changed from simply supported to hinged, BC2, by allowing the edges of the panel to rotate but not translate or $u_{x,}=u_z=0$ along the edge $x=a/2$, and $u_y=u_z=0$ along the edge $y=b/2$. Changing the boundary conditions to clamped, BC3, or $u_x=u_y=u_{z,}=0, \theta_x=\theta_y=\theta_z=0$ along the edge $x=a/2$, as well as along the edge $y=b/2$ is shown in Fig. 5. The boundary conditions have a large effect on the deflection of the panel. The 12.7mm thick core with BC1 is on top of the 25.4mm thick core with BC2 which is

important because thinner cores are usually affected more by curvature than thicker cores for every other condition shown.

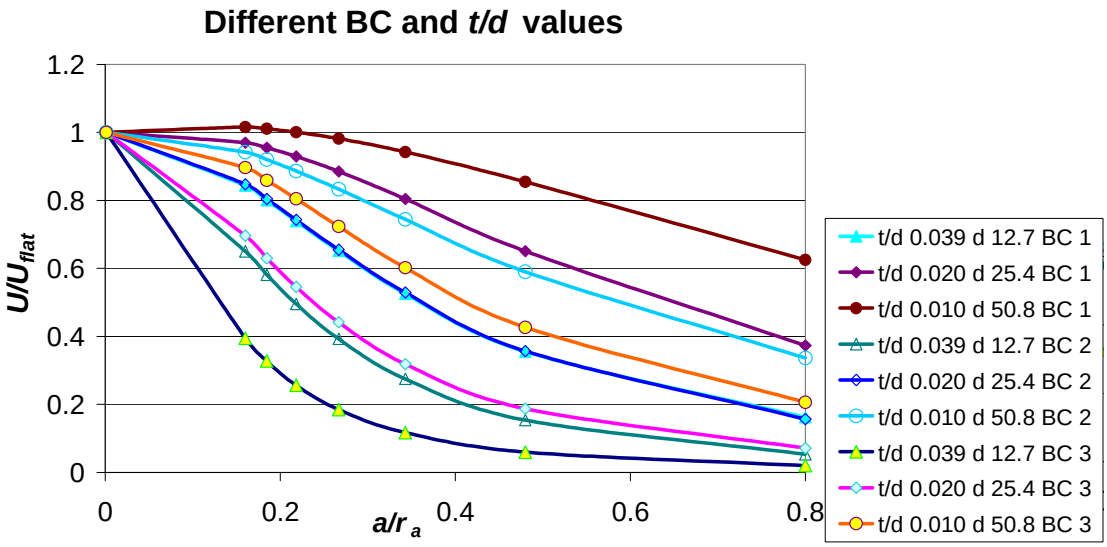


Fig. 5. Comparison between Boundary Conditions (BC) and *t/d.*

In Fig. 6 there is a comparison between different face sheet thicknesses over three different core thicknesses all with the ratio, E_s/E_c of 324. It appears that a thicker face sheet has a bigger effect on thicker cores compared to thinner cores.

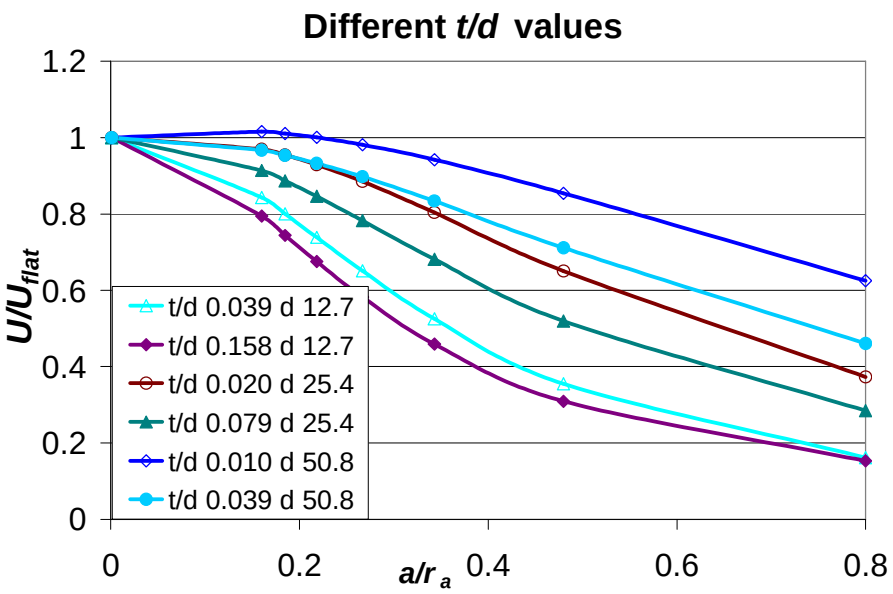


Fig. 6. Varying skin thicknesses for each core thickness.

Fig. 7 shows the effect of changing the aspect ratio from a square to a rectangular panel while the ratio, E_s/E_c is 324. The value of *a* is fixed at 0.6m and *b* changes. The ratio listed for each curve is the ratio of the panel width divided by its length, *b*/*a*. For example, the point [0.48,0.70] on the graph corresponds to curve *t/d* 0.01 H80 d 0.0508 ratio 2 has a face sheet thickness, *t*, of 0.5mm, an H80 foam core thickness, *d* of 50.8mm, a r_a=r_b of 1.25m, an *a* of 0.6m, *b* of 1.2m. For the case shown in fig. 7 with *a* being constant and r_a=r_b making the panel longer in one direction makes the curvature have a greater effect on the stiffness.

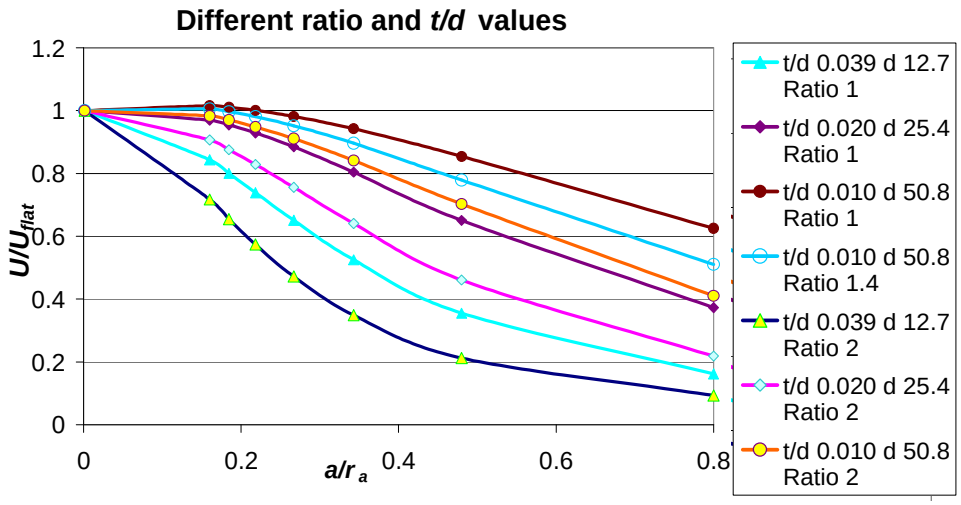


Fig. 7. Different length to width ratios.

Fig. 8 shows the percent deflection by taking the maximum deflection and dividing it by the shortest panel side for different face sheet and foam core types and foam core thicknesses. It can be seen how thinner cores are influenced much more by curvature than thicker ones.

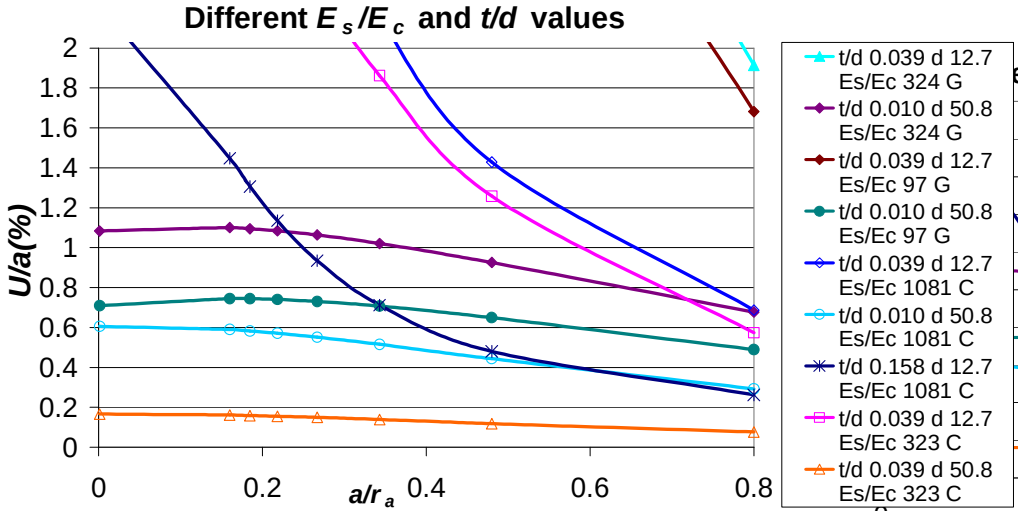


Fig. 8. *U/a* vs. a/r_a.

From the results of the parameter study, a better understanding of panel behavior was obtained which led to further FEA analysis using a more detailed FEA model followed by the selection of the panel design to be tested experimentally. Design requirements of a hydrostatically pressure loaded panel were implemented to select a panel design. Once the panel design was selected, the testing fixture could be analyzed. The panel and fixture design are discussed in the next two sections.

Design of Panel for Experimental Investigation

The design requirements of a pressure loaded ship hull panel may include a stiffness requirement and some strength requirements. The stiffness requirement may be that the maximum deflection is less than, say, 2% of the length of the shorter side of the panel. The strength requirements may be that the shear stress in the core is less than the allowable shear strength, that the tensile strains anywhere in the skins are less than the tensile failure strain of the face skins, and that the compression strains in the skins are less than both the compression failure strain and the wrinkling strain. At present the 2% deflection requirement was used. The shear strengths of the cores were taken from the manufacturer (Diab Inc.) and are given in Table 1. The failure strains of the skins were assumed to be 1.3 % in tension and 1.3 % in compression. The wrinkling strain may be estimated by the Hoff and Mautner [18] wrinkling formula:

$$\sigma_{wr} \approx 0.5(E_S E_C G_C)^{1/3}$$

$$\varepsilon_{wr} \approx \frac{\sigma_{wr}}{E_S} \approx 0.5\left(\frac{E_S E_C G_C}{E_S^3}\right)^{1/3} \qquad (4)$$

$$\approx 0.5\left(\frac{E_C^2}{E_S^2 * 2(1+\upsilon_C)}\right)^{1/3}$$

Where σ_{wr} is the wrinkling stress, ε_{wr} is the wrinkling strain, and υ_C is the Poisson's Ratio of the core. The criterion varies with foam core density but the two that were considered, Divinycell H80 and H100, give wrinkling strains of 0.9% and 1.1%, respectively.

There may be further requirements on impact, in particular on the outer skin of a ship hull. This typically leads to thicker skins on the outside than on the inside of the sandwich panels. At present, explicit impact requirements were not included but the outer skin was forced to be 50% thicker than the inner skin. This is reasonable for many applications.

Panels were initially modeled as described in the parameter study above, i.e., modeling only the panel (no steel fixture or other complex support), assuming simply supported edges, and using 2D shell elements. The experimental design panel model had additional detail. The tapered foam core where the inner and outer skins came together to a single skin was added to the model along with reinforcement layers and orthotropic GFRP face sheet properties, Table 2.

Table 2. Anisotropic material properties used in Ansys.

Ex	22	GPa
Ey	22	GPa
Ez	5.5	GPa
Gxy	4	GPa
Gxz	2	GPa
Gyz	2	GPa
PRxy	0.275	-
PRxz	0.275	-
PRyz	0.275	-
Dens	1800	kg/m^3

The lightest panel configuration that fulfilled the design requirements on stiffness, core strength and skin strength had the following parameters: curvature r_a=r_b =0.75m, 0.75 mm outer skin, 0.5 mm inner skin,18 mm H80 foam core, and 2.25mm thick flange where the foam core tapers to a single skin. This panel configuration was chosen as the final panel to manufacture and experimentally test under hydrostatic pressure, Table 3. The properties of this panel were used to design the steel fixture for testing which is discussed in the next section.

Table 3. Properties of panel chosen to be manufactured.

Density (kg/m^3)	**Outer skin (mm)**	**Inner Skin (mm)**	**Core (mm)**	**R**	**Max *z*-Deflection (mm)**	**Mass (kg)**
80	0.75	0.5	18	0.75	11.0	1.283

Fixture Analysis

The previously mentioned fixture to attach to the panel for testing was designed using Solidworks 2006 educational version and analyzed using Cosmosworks 2006 educational version. A quarter of the fixture and a homogenized sandwich panel that was modeled using shell elements. The bolt holes were constrained to have no displacement, and symmetry boundary conditions were applied to the planes of symmetry at $x = 0$ and $y = 0$, respectively. In summary, the boundary conditions were $u_x=u_y=u_y =0$ at the bolt holes; $u_x=0$ and $\theta_y=\theta_z=0$ along the edge $x=0$; and $u_y=0$ and $\theta_x=\theta_z=0$ along the edge $y=0$. The "bond plate" to which the sandwich panels were adhesively bonded was given the properties of AL-6XN stainless steel whereas the rest of the test fixture was given the properties of mild steel. There were no sandwich elements available for the analysis using Cosmosworks, instead, the sandwich panel was modeled as a homogeneous material with a modulus and thickness such that it had the same in-plane stiffness and bending stiffness as the previously mentioned sandwich panel designed to be experimentally tested. The following two approximate formulas were used to calculate the material properties and thickness of the homogenized panel:

$$E_{\text{hom}} * h_{\text{hom}} = E\ (t_1 + t_2)$$
$$E_{\text{hom}} * \frac{h_{\text{hom}}^3}{12} = (t_1 h_1^2 + t_2 h_2^2) E \qquad (5, 6)$$

E_{hom} and h_{hom} are Young's modulus and the thickness of the homogenized material, E is Young's modulus of the fiberglass, t_1 and t_2 are outer and inner skin thicknesses, h_1 and

h_2 are the outer and inner distances from the midline of the outer and inner skins to the neutral axis. The calculated E_{hom} and h_{hom} of the homogeneous material equivalent to the designed sandwiched panel were 0.87 GPa and 32 mm respectively. These equivalent material properties were used in the analysis of the test fixture. A summary of material properties used in the fixture analysis is given in Table 4.

Table 4. Fixture analysis properties.

Part	Thickness (mm)	Material	Ex (GPa)	PRxy	Density (kg/m3)
Bottom Plate	9.5	Carbon Steel	210	0.28	7800
Wall Plates	4.8	"	"	"	"
Bond Plate	2	AL6XN	195	0.28	8060
GFRP Flange	2.25	Fiberglass	22	0.275	1800
Homogeneous Material	32	Homogeneous	0.87	0.3	1000

The test fixture Finite Element analyses in COSMOSWorks used a pressure of 300kPa, twice the design load, applied normal to the surfaces of the panel, the fiberglass flange, and outer plates. The COSMOSWorks FFEPlus solver was used and results verified that the fixture would not reach the material's yield stress. In order to make the fixture lighter and easier to transport, the actual fixture had a 4.8mm thick bottom plate with a 12.7mm thick bolt plate instead of the 9.5mm thick bottom plate as used in the analysis. Making two plates instead of one was done so the fixture was lighter and easier to transport and the thicker bolt plate reduces the deformation of the fixture under higher pressures. The side plates were MIG welded to the bottom plate. The bond plate was

formed to the curvature of the sandwich panel and welded. It should be noted that the bond plate overhung the inner wall plate by 5mm to improve weldablity. The overhang was not ground flush with the inner wall plate in an attempt to slightly reduce a stress concentration at the interface and create a small stiffness gradient. By making the stainless steel bond plate overhang a small amount, there is the high stiffness box beam transitioning to a thin, unsupported piece of stainless steel, to a single fiberglass skin. The welded fixture is shown in Fig. 2.

The designed panel for testing was manufactured, followed by the steel test fixture. They were then joined and tested under hydrostatic water pressure which is discussed in the following sections.

Manufacturing of doubly curved sandwich panels

In order to fabricate the panel with properties listed in Table 3, a doubly curved mold with a radius of curvature of 0.75m needed to be made. Several methods for making molds were studied. The requirements were that the mold material should be inexpensive and easy to transport, the mold should be easy and inexpensive to machine, the geometric tolerances should be good, the mold should be non-metallic, and it should be compatible with vinyl ester such that panels could be vacuum infused directly in the mold. Considering the requirements and facilities at hand, Renicell E320 polycarbamate foam from Diab Inc. was chosen for the mold material. This is an inexpensive, easy to

machine material with a density of 320 kg/m^3. It can be obtained in blocks thick enough for the present panels. The mold was designed using Solidworks to have the same curvature as the doubly curved panel, and large enough to lay up materials, infusion and vacuum hoses, etc. and fit a vacuum bag. The Renicell was machined in-house using a 5-axis CNC router, Fig. 9.



Fig. 9. CNC machining of mold.

The foam cores for the sandwich panels needed to be formed to have close to the same curvature as the desired finished panels for testing (r_a=r_b=0.75m, eq. [1]). This was due to the significant curvature and test trials indicated a flat foam core could not be successfully vacuumed down to the mold, infused, and maintain the desired geometry. In principle, one could machine the foam core from a 125mm thick block of foam, but it

would be very expensive and quite cumbersome. Another option was to machine the foam core to the correct flat size, soak it in acetone until it became soft, vacuum the softened foam core to the curved mold surface, and hold under vacuum until the acetone evaporated from the core. This method shapes the foam core very nicely but the effects of acetone on the foam core properties are not fully known [20]. Rather, the foam cores were formed by first machining the flat foam cores, then applying heat until they softened, and then vacuuming them down to the mold and let cool. The 18mm thick foam cores were machined with 45° beveled edges with 55mm corner radii, 15mm radius fillets on top of the bevels, and 2x2mm infusion grooves spaced 25mm apart machined on the top and bottom. These machined cores were thermoformed by heating with IR heaters, placed into the Renicell mold, and vacuumed until cooled. After several trials to fine tune the process, the foam core conformed very nicely to the mold with very little springback. The thermoforming presumably leads to no noticeable change in core/face sheet adhesion and only a small change in structural properties [21].

The face sheets consisted of three different types of glass fiber reinforcements; Hexcel 7725 which is a 2/2 twill with a surface weight of 298 g/m^2, Owens Corning Knytex WR24-5x4 woven roving at 815 g/m^2, and Owens Corning M-8610 continuous filament mat at 450 g/m^2. The Hexcel was used as the inner and outer skins as well as reinforcement layers around the tapered portion of the foam core. The woven roving and the continuous filament mat were used to thicken the flange in order to improve the strength close to where the panel was bonded to the test fixture. The continuous filament mat was also used as resin flow medium. The woven roving fabric had a fabric

weight of 815 g/m^2, with 440 g/m^2 in the 0º direction and 375 g/m^2 in the 90º direction. The material properties are shown in Table 5 [22]. The matrix was Ashland Derakane 8084 vinyl ester epoxy resin, mixed with Cobalt Naphthenate-6% (CoNap), Dimethylaniline (DMA), Methylethylketone peroxide (MEKP), and 2, 4-Pentanedione (2, 4-P). The CoNap and DMA promote the reaction, MEKP is the hardener, and 2,4-P is an inhibitor used to increase the gel-time. The weight percentages added of each chemical recommended by the manufacturer for 80 ºF are as follows: 1.5% MEKP, 0.025% DMA, and 0.15% CoNap [23]. When 2,4-P is added, more CoNap is recommended and therefore 0.2% CoNap was used. The amount of 2,4-P generally varies between 0.13% and 0.5% depending on the desired gel time. At present, 0.14% of 2,4-P was used to give roughly a 3-4 hour gel time.

Table 5. WR24-5x4 Knytex glass fiber typical material properties [4].

Material Properties of Laminate based on 50% glass content by weight		
Tensile Strength	MPa	289
Tensile Modulus	GPa	14.3
Compression Strength	MPa	230
Compression Modulus	GPa	15.7
Flexural Strength	MPa	385
Flexural Modulus	GPa	15.2

-Panel lay-up

In order to successfully manufacture the doubly curved foam core and infused sandwich panel to the determined design, two panels were made to shakedown the manufacturing process and testing. The doubly curved panels were made by first laying the dry glass fiber into the previously mentioned Renicell high density foam mold. However, vinyl ester adheres to Renicell foam. A protective surface was made by covering the mold with vacuum bag and evacuating the air. The vacuum bag was challenging to make to conform to the doubly curved mold surface with no wrinkles. When wrinkles did form, they were pushed to the edges of the mold to leave a smooth mold surface. Three layers of Hexcel 7725 bi-directional fabric were laid in the vacuum bagged mold to make the outer skin, and then the thermoformed foam core was positioned on top of the outer skin layers, followed by the inner two layers of Hexcel 7725, Figs 10-12.

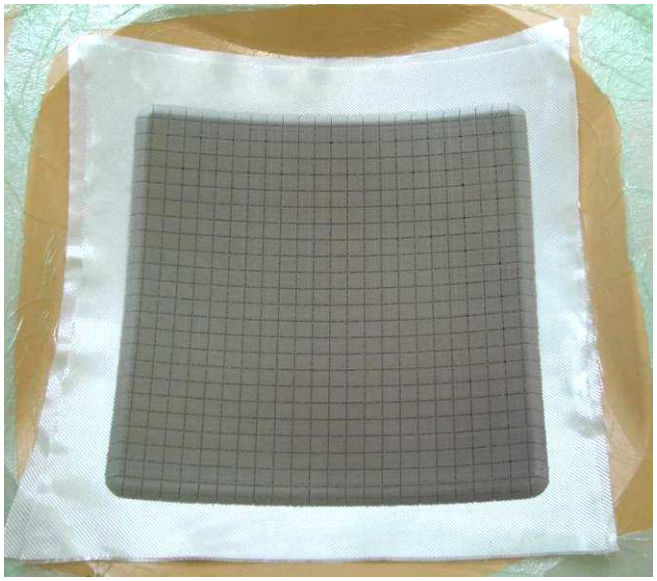


Fig.10. Thermoformed foam core in mold.

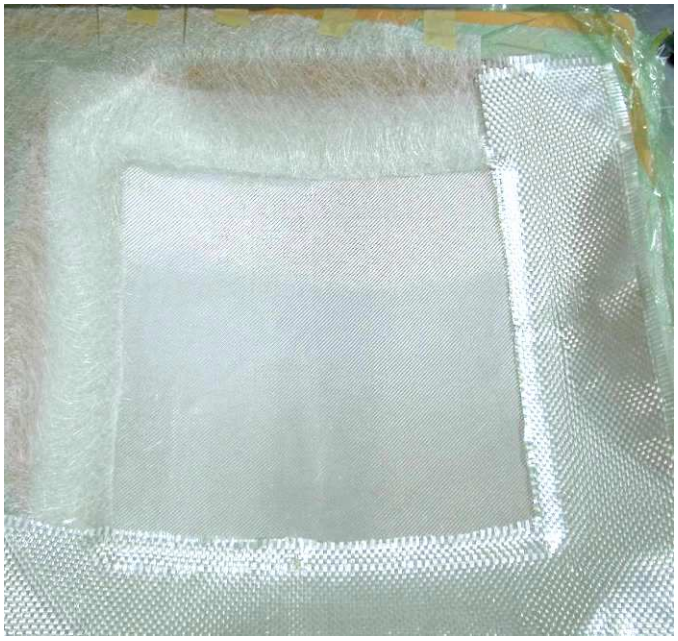


Fig.11. Thickening layers of WR-24 and CFM.



Fig. 12. Laying up the reinforcement layers.

In order to make the single skin flange thick enough to withstand the loading, a thickener layer was added. This thickener layer consisted of one layer of continuous filament mat on the side closest to where the resin was introduced and two layers of WR-24 on the opposite side, Fig. 11. Reinforcement layers of Hexcel 7725 were then laid over the thickener layers to transfer the load up the beveled edges. The three reinforcement layers were staggered by 15mm, starting at 45mm from the edge of the top of the bevel, Fig. 12.

After the fiber reinforcements of the inner skin had been laid down, the complete panel was covered with peel ply and breather. The former was used so the breather can be removed from the part after cure, and the latter was used to entrap air bubbles from any leaks during infusion as well as to promote saturation of the fiber reinforcements. Resin distribution medium was used on top of the breather from the infusion tubes to the bevel along two edges of the panel. The lay-up was then covered with a vacuum bag and evacuated of air, Fig. 13. In order to reduce the risk of air leaks further, the bagged part was covered with breather and another vacuum bag and evacuated of air (not shown).

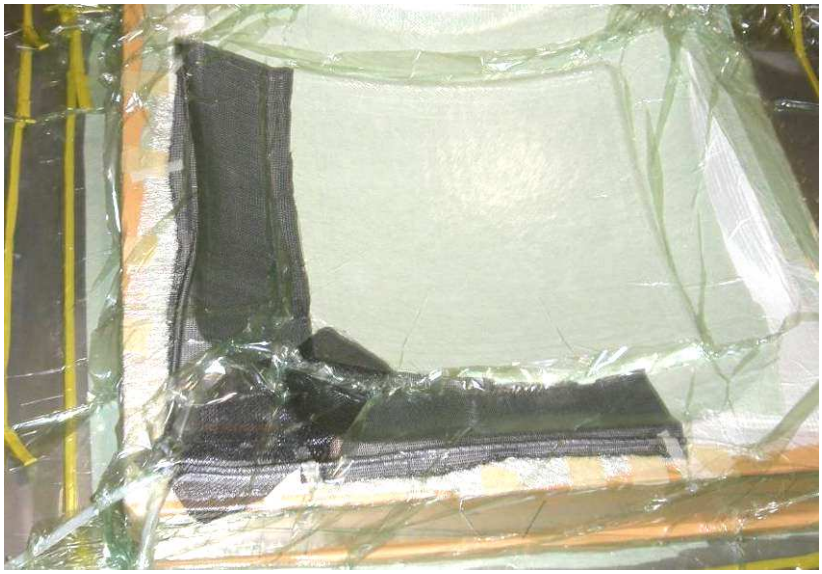


Fig. 13. Vacuum bagging.

The vinyl ester resin was mixed for 5 minutes, degassed for 15 minutes and then the resin was infused through the dry fibers by vacuum. It took approximately 35 minutes to infuse a panel. After the infusion had completed the resin line was then closed off and the pressure under the vacuum bag was allowed to equalize. The vacuum pressure was then slowly reduced using a vacuum regulator, from essentially pure vacuum to 25kPa absolute pressure, to reduce the chances of the vinyl ester boiling. The part was left under vacuum for 24 hours and then demolded and trimmed to the correct size using an abrasive waterjet cutter, Figs. 14 and 15. Each panel was then instrumented and the surface was prepared for bonding as described below.

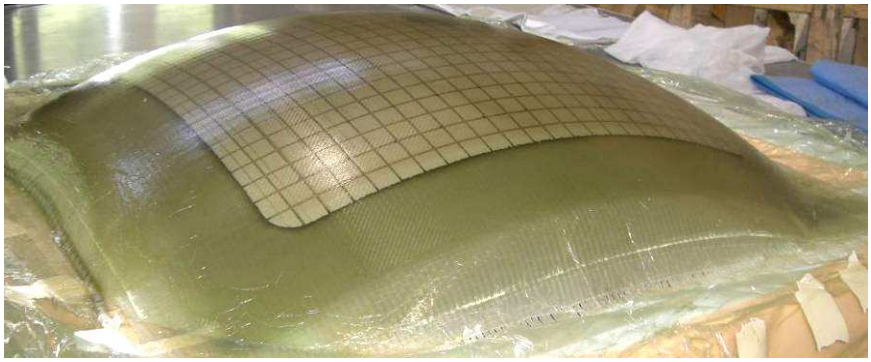


Fig. 14. Demolded part.

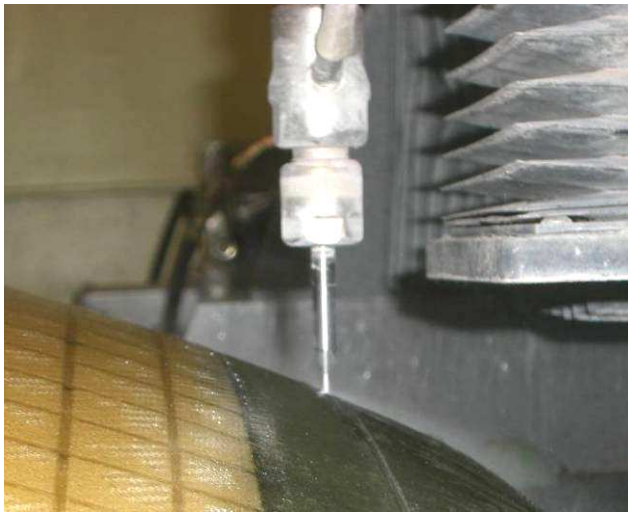


Fig. 15. Waterjetting to size.

-Panel Preparation

The final doubly curved test panel was instrumented with eight Vishay CEA-06-500UW-350 strain gages. The shakedown panels were instrumented with one strain

gage at the center of each panel on both the inner and outer skins. The strain gages were bonded to the final panel in eight locations, four on dry (inner) skin and four on wet (outer) skin. Vishay's recommended surface preparation and bonding techniques were followed [24]. The locations of the strain gages and their labels are shown in Fig. 16. The instrumented panels were then prepared for bonding to the test fixture.

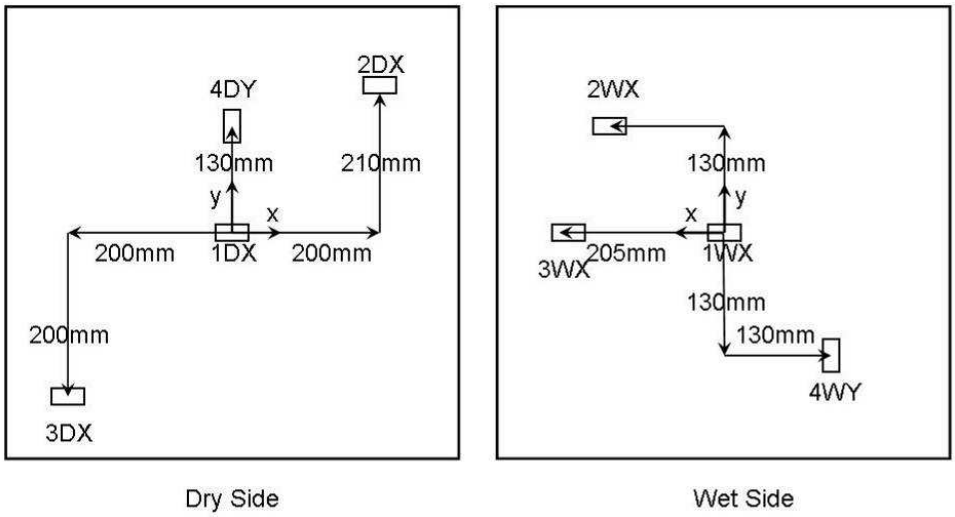


Fig. 16. Strain gage location and label.

Surface preparation is extremely important for the panel's performance and care was taken to promote a good panel/fixture bond [25]. The fixture's stainless steel bonding surface was prepared by grit blasting and thoroughly cleaned with trichloroethylene. The panel bonding surface was carefully sanded using 80 grit sand paper and then thoroughly cleaned with trichloroethylene. An epoxy paste adhesive, SIA E2119 A/B, was used to bond the panel to the fixture. E2119 is a 1:1 two-part toughened epoxy

adhesive that will achieve handling strength in less than 8 hours and full cure in 72 hours at room temperature [26].

The SIA epoxy adhesive was applied, using a pneumatic gun with a static mixing nozzle, to the fixture and panel and evenly spread over the bonding surfaces. An extra bead of epoxy was applied down the middle of the bonding surface to assure a sufficient bond line thickness and to make sure excess epoxy forced out any air when the panel was mounted to the fixture. The panel was placed on the steel fixture and fixed with duct tape, then turned over and placed in a CNC machined bonding jig. This jig had the doubly curved shape of the panel, but touched the panel only by the bonding surface. The jig was made of relatively soft Styrofoam which allowed for an even clamping pressure, Fig. 17. The steel jig was then weighted down with lead and left to cure. The adhesive cured for 14 hours while wrapped in an electric blanket, elevating the temperature to about 35C, then post-cured for 1.5 hours at 70C.



Fig. 17. Panel epoxied to fixture in Styrofoam jig.

After the epoxy was sufficiently cured between the panel and fixture, wire leads were attached to the previously installed strain gages and secured to the panel using silicon. The panel and fixture was then attached to the testing tank. To prevent leaking, a rubber gasket was placed in between the test tank and fixture and another gasket in between the fixture and bolt plate. Loctite 567 was applied to all bolts.

Testing

The curved panels were tested under hydrostatic loading at the Hybrid Structures Lab at the University of Maine. The instrumented panels, bonded to the test fixture which was bolted to the test tank, were repeatedly loaded and unloaded under increasing pressure until final failure.

-Test Tank Design

The test tank was designed and manufactured at the University of Maine. The steel test fixture was designed to withstand 300 kPa water pressure, or twice the panel design load of 150 kPa, without yielding. The test tank was designed for 450 kPa. The fixture, test tank and all connections were watertight. The tank consisted of MIG welded 835x240x25mm steel plates making up the walls, 835x76x12.7mm steel plates making

up the top, and a 1090x1090x12.7mm steel plate for the bottom. In order to provide adequate stiffness to the sides and the bottom flanges, 240x101x9.5mm web stiffeners were welded onto the sides on 209mm centers. The tank was bolted to a stiffened 50mm thick steel plate to provide stiffness for the tank bottom. The top flange was drilled and tapped matching the bolt pattern of the test fixture. The overall dimensions of the tank can be seen in Fig. 18.

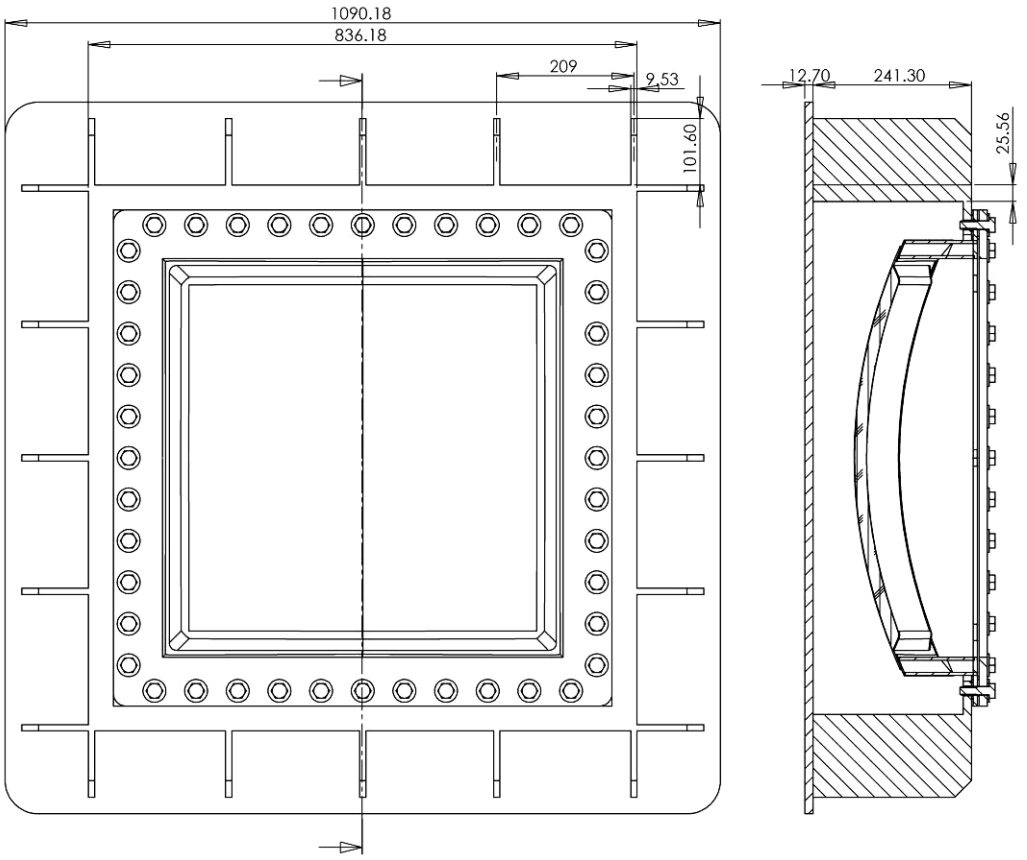


Fig. 18. Test tank schematic.

-Instrumentation

The panels were instrumented with one linear variable displacement transducer (LVDT) at the center of each panel and eight metal foil strain gages. The applied pressure was measured using an Omega PX303 pressure transducer. Silicone was used to protect the solder joint from straining during panel installation and from the water pressure. The wire leads were soldered to cables connected to the data acquisition system and heat shrink was used to protect the solder joint during testing.

Data acquisition was carried out using a Pentium 4 computer with an IOTECH Daq-board 2000 card, and Vishay 2120 multi-channel strain signal conditioner. The system had 16 bit analog-to-digital conversion resolution and was capable of reading a total of 48 channels at a rate of 1 kHz, which was more then adequate for the present test. The data acquisition process was controlled using the DAQFI_D5 software, written at the University of Maine.

-Testing Method

The doubly curved panel was tested at University of Maine's Hybrid Structures Laboratory, located in the Advanced Manufacturing Center using the previously described hydrostatic tank. An air-over-water method was used to load the panel due to its simplicity, safety and relatively low cost. It also allowed use of the laboratory's

existing 827 kPa air supply. A 984-L pressure vessel, filled with water was the interface between the test tank and the compressed air. In order to insure that no initial hydrostatic pressure was developed the vessel was filled to a height equal to the top of the test tank. A Control Air, Inc 700 precision, manual regulating valve was used to achieve the desired pressure level, by manually dialing in each pressure step, Fig. 19. A picture of the test setup is shown in Fig. 20.

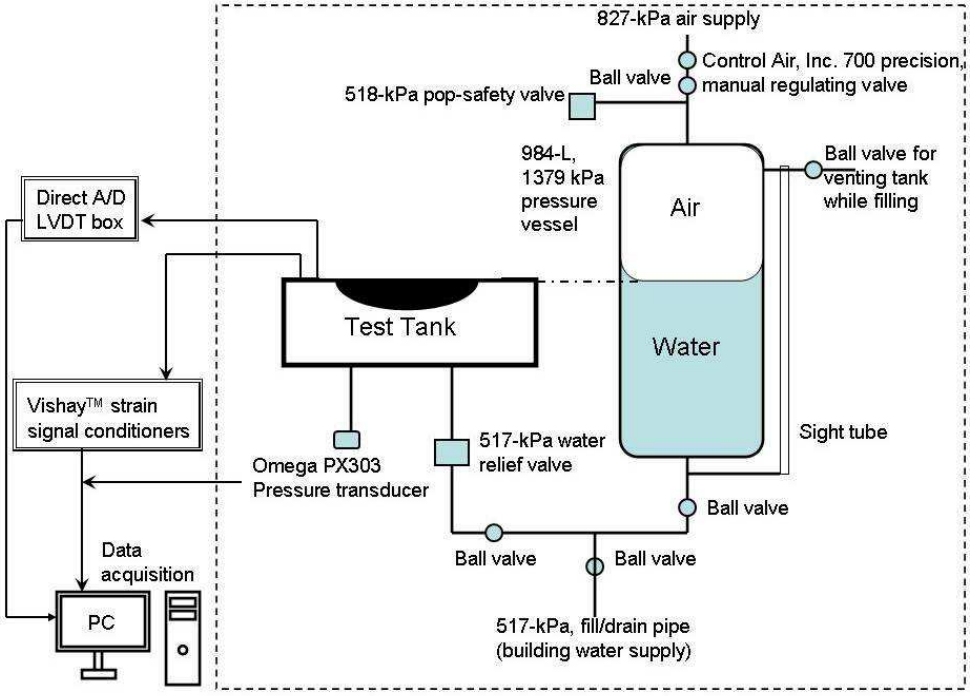


Fig. 19. Schematic of test setup.

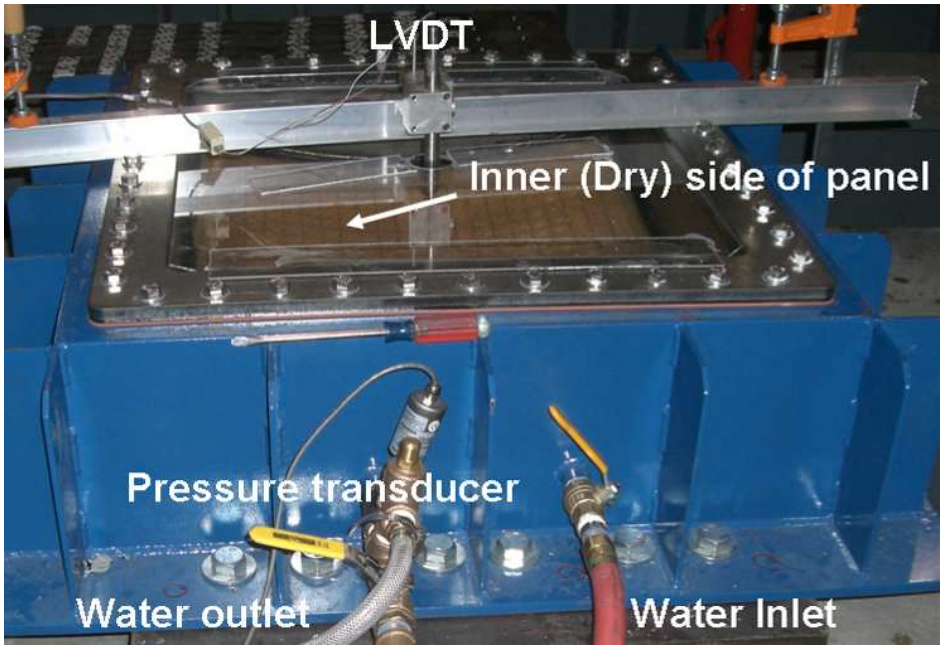


Fig. 20. Testing setup.

Two shakedown tests were preformed to test the data collection, instrumentation, and connections between the panel, fixture, and test tank. After the two successful shakedown tests, testing of the final panel assembly was conducted in a cyclic fashion. Cyclic testing was used to study the degradation of the structural system due to repetitive loading cycles and to assess the load level at which the onset of damage occurred. The test was composed of a total of five cyclic increment sets as shown in fig. 21. Each cycle set was comprised of two equal load cycles. The pressure was increased by equal increments of 40kpa until the design load was reached. After the design load was reached the pressure was increased by smaller increments up to 130% of the design

load. The panel assembly was then tested to failure at 175% of design load. Load, displacement and strain data were recorded throughout the test.

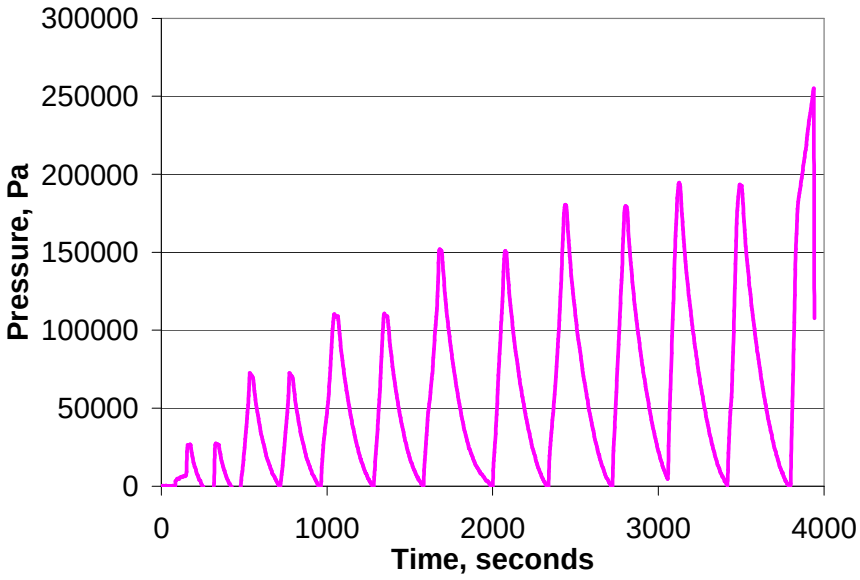


Fig. 21. Pressure History Plot.

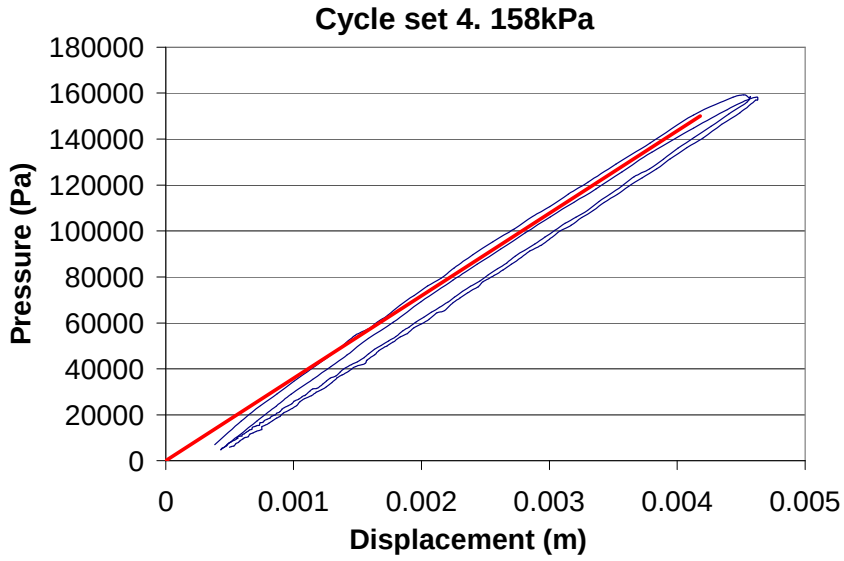
Results

The results of the hydrostatic pressure test are summarized in Table 6 for the design pressure of 150kPa. Central deflection and strains at various locations are provided.

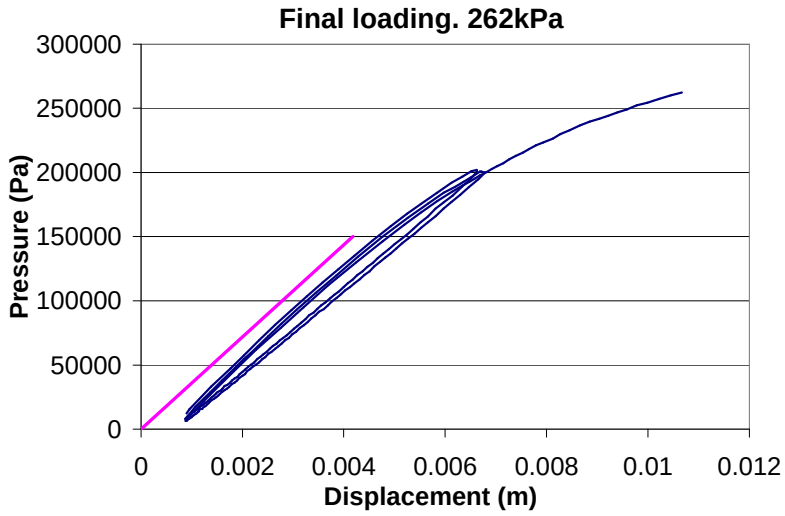
Table 6. Percent difference between Ansys and test results.

	Ansys	Test	Difference (%)
Center Deflection (mm)	4.18	4.13	1.2
Strain gages (microstrain)			
S1DX	-1362	-1351	0.8
S2DX	228	No data	-
S3DX	164	No data	-
S4DY	-616	-726	16.4
S1WX	-2318	-2260	2.5
S2WX	-2192	-2058	6.3
S3WX	-2143	-1979	8.0
S4WY	-2232	-2606	15.5

Table 6 shows the values the LVDT and strain gages recorded during the test, the Ansys predicted results, and the percent difference between them. The Ansys predicted results are from the model with the entire fixture included in the analysis. Representative load verses displacement graphs are shown in Figs. 22a-b.



a)



b)

Fig. 22a-b. Load verses displacement curves for design and final loading.

The graphs correspond to center point deflection of the panel measured by the LVDT verses the pressure recorded by the pressure transducer. For clarity, only the design load (fourth) and the final load steps are shown. The fourth load step was to the design load of 150 kPa. Each graph shows close to linear behavior. There is some hysteresis which may be due to mechanical connections (rubber gaskets, bolts, etc moving slightly) and/or microcracks forming in the composite skins upon loading. The maximum displacements at peak load were 4.1mm and 10.7mm, respectively, for the fourth and the final load steps. The Ansys model predicted a centerpoint deflection of 4.2mm for the design load of 150kPa. 'Pings' typical of damage in composites were heard during the 5^{th} and 6^{th} load steps for the first time, and several more times before panel failure. During the testing, no leaks or visual damage were noticed in the panel, fixture, or test

tank until final panel failure when water came rushing through the panel. The panel went from showing no sign of damage, except that several pings were heard, to complete failure so quickly it was difficult to determine the exact mode of failure or failure progression. The top and bottom of the panel after failure are shown in figs. 23 and 24.

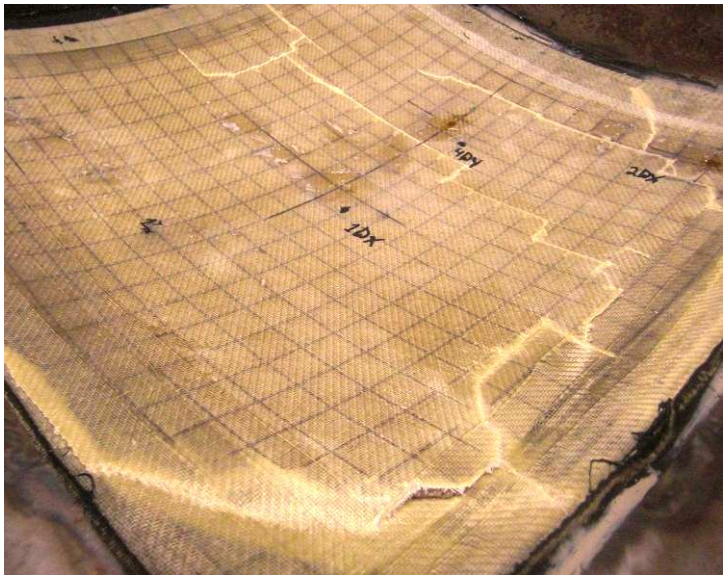
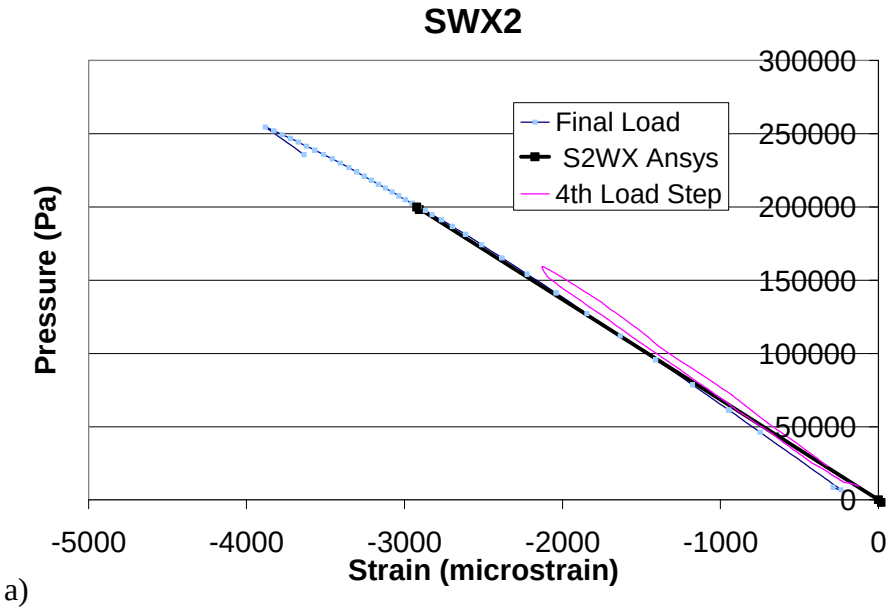


Fig. 23. Damaged Dry side.

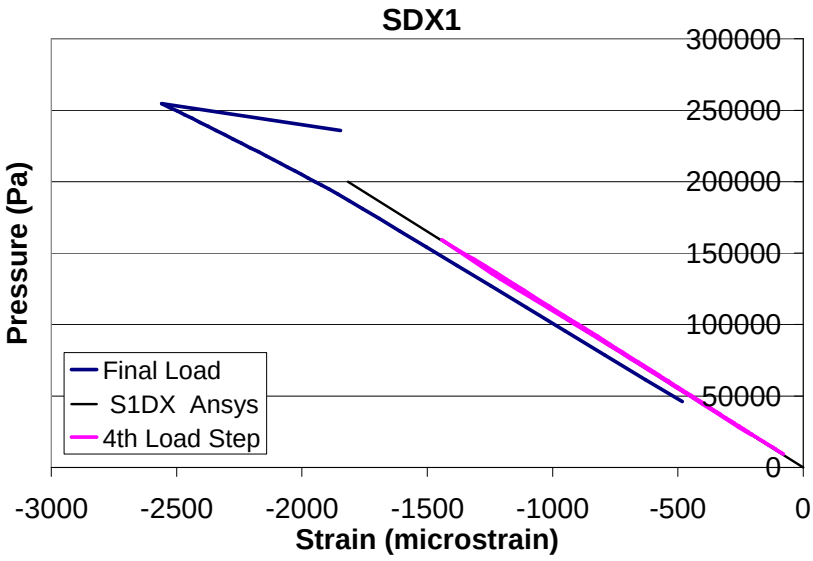


Fig. 24. Damaged Wet side.

Representative load verses strain curves are shown in figs 25a-b for the strain gages SWX2, located on the outer (wet) side 130mm in the x and y direction from the center of the panel and SDX1 located on the inner(dry) side in the center of the panel. The recorded strain gage data showed good agreement with Ansys Finite Element results which are also plotted in Figs. 25 a-b.



a)



b)

Fig. 25a-b. Load verses strain for strain gage SWX2 and SDX1.

Based upon material coupon tests, a failure strain of 13,000 microstrain in tension and 9,200 microstrain in compression (wrinkling) was estimated for the composite panels. A maximum strain of 4,200 microstrain in compression was recorded by the strain gage at the bottom of the outer skin designated, WX1, which was considerably smaller than

the predicted failure strain. This is believed to be due to the inherent waviness and thickness variation of a woven fiber reinforcement. The thickness variation reduces bending stiffness to a much larger extent than it reduces in-plane stiffness [27]. An appropriate wrinkling formula would use bending stiffnesses rather than in-plane stiffnesses, as was used in eq. (4). The low failure strain may also be due to the fact that draping the fabric on a doubly curved surface causes the fibers to be misaligned.

Chapter 3

LARGE STEEL/COMPOSITE HYBRID BEAM. PART I: DESIGN AND MANUFACTURE

By combining traditional steel manufacturing with modern composite construction a hybrid ship structure can be designed which draws on the advantages of both materials. Composites are known for their high strength-to-weight, fatigue and corrosion resistance, moldability and excellent thermal and sound isolation. Likewise, steels are recognized for their high stiffness, ductility, isotropy, weldability and the relative ease and familiarity of their use for both design and manufacture. Together these materials hold potential for building a novel structure, which is superior in certain aspects to traditional steel ship designs.

Several different hybrid ship structures have been proposed. One concept is to use lightweight composite structures for the bow and stern, where the bending loads are low, and to use more traditional steel construction to take the higher bending loads in the ship's center section [28-30]. Another concept, called MACH, (Modular advanced composite hullform) was developed for lifting bodies and utilizes a steel "rib-cage" which has relatively small panels attached to it [9]. Still another concept is to use a full steel truss with all sides enclosed by large composite panels.

Previous work by Grenestedt and co-workers considers a hybrid truss structure falling into the latter category [14-16]. This work considered a five-sided ship hull cross section, having a steel frame designed to take the global bending loads, and bonded fiberglass sandwich panels designed to take shear and water pressure loads. Wave induced loads were calculated using the American Bureau of Shipping (ABS) guidelines for a 142m (water line length) destroyer class ship, and applied to a 1:35 scale model. This model had a constant cross section and it was tested in a six-point bending setup. The model exhibited excellent global ductility, something that would not be expected from an all-composite structure. The beam was tested to 36% above the design load, which resulted in yielding within the steel truss and permanent global deformation but otherwise no damage. In particular there were no failures within the composite panels or bonded joints.

The present chapter seeks to extend this work by testing a much larger 1:8 scale hybrid truss. This beam was constructed in a manner similar to the previous 1:35 scale model (i.e. steel taking the global bending loads, and bonded composite panels taking the shear loads). The structure was subjected to cyclic loading in order to shed light on the fatigue performance of this concept for steel/composite ship hulls.

Structural Design

The design of the present hybrid beam originated from an all-steel beam by Maglev Inc. (McKeesport, PA, USA), intended as a bridge girder for magnetically levitated trains. This design was modified and retrofitted for the purpose of testing the beam as a 1:8 scale model of a destroyer class ship hull, Fig. 26. Several major modifications were made to the original design. Adhesively bonded composite sandwich panels replaced the vertical steel webs at the center of the beam, making a hybrid steel/composite structure with reduced weight. The "window frames" to which the composite panels were bonded were made of AL-6XN (Allegheny Ludlum Corp., Brackenridge, PA, USA) superaustenitic stainless steel, a candidate material for future ship hulls. Bonding procedures for composites to AL-6XN have been investigated in previous research. The remainder of the structure remained carbon steel.

Box beams were added to the steel girder in both the transverse and longitudinal directions in order to make the structure more similar to the previously studied 1:35 scale model [14]. The resulting steel truss is shown in Fig. 27 with cross section dimensions given in Fig. 28.

Figure 29 shows a cut-away view exposing the internal structure of the beam. Upper and Lower Deck plates were made of A36 carbon steel 18mm and 40mm thick, respectively. The essentially vertical web plates at the ends of the beam were made from 12mm carbon steel. Towards the center of the beam, surrounding the composite

panels, the web plates were substituted by "window frames" of 12.7mm thick AL-6XN stainless steel. The longitudinal box beams were constructed by welding L-shaped carbon steel angle stock (152mm base length and 19mm thick) to the deck, bottom and web plating. The vertical and transverse box beams were fabricated from 12mm thick carbon steel plate.

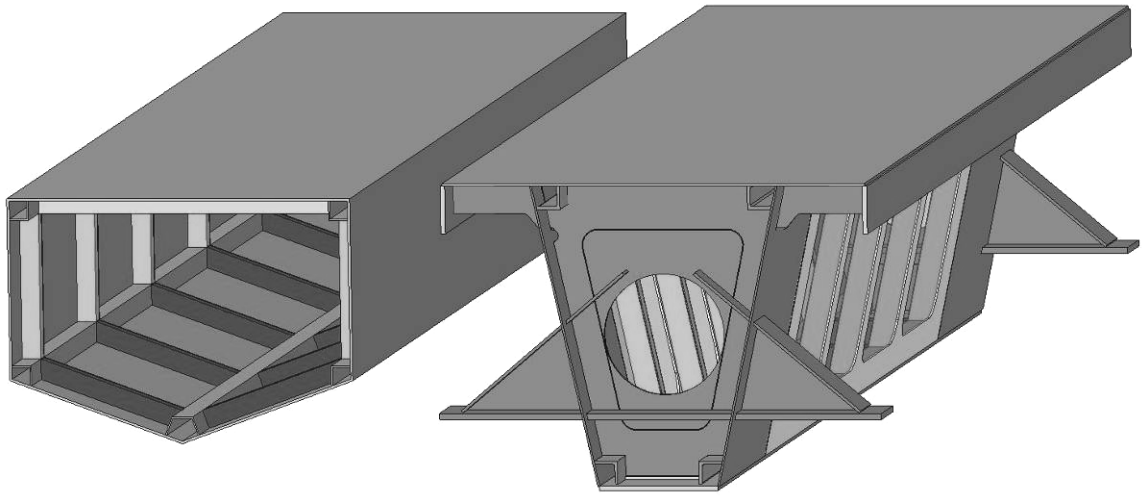


Fig. 26. Scaled down (1:8) destroyer (left) next to the presently studied beam (right).

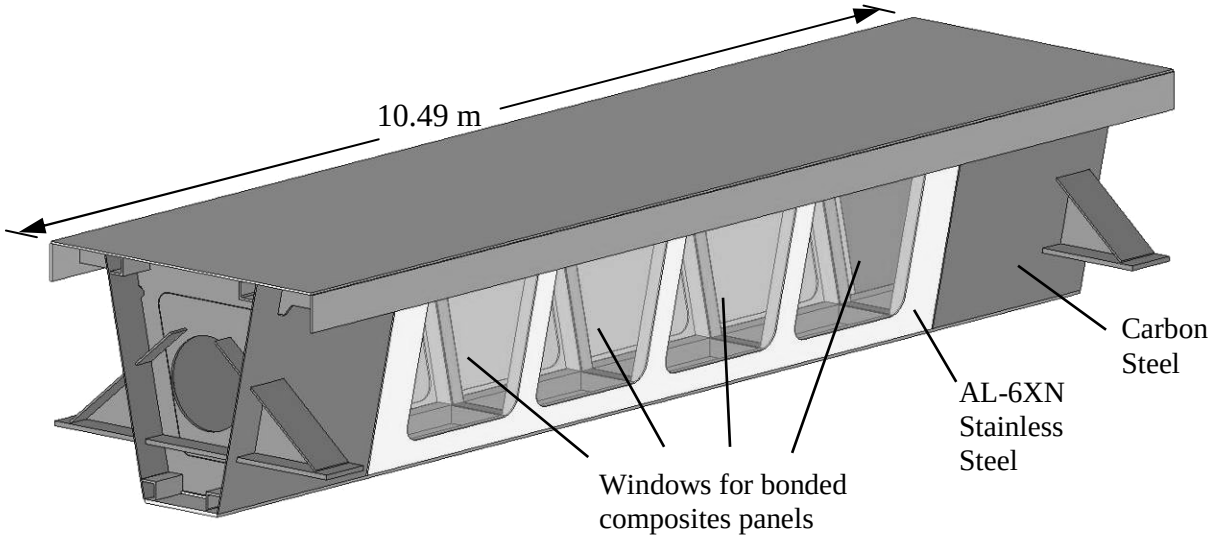


Fig. 27. Steel structure of specimen.

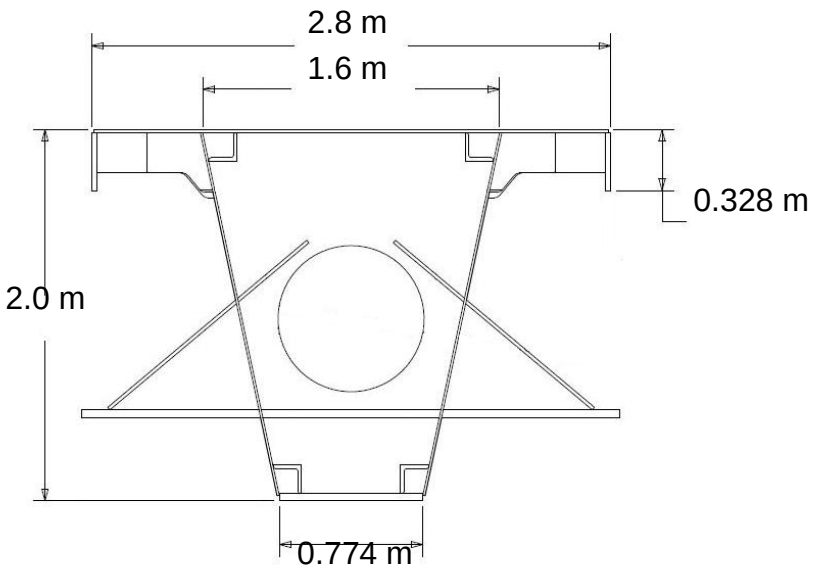


Fig. 28. Cross section dimensions.

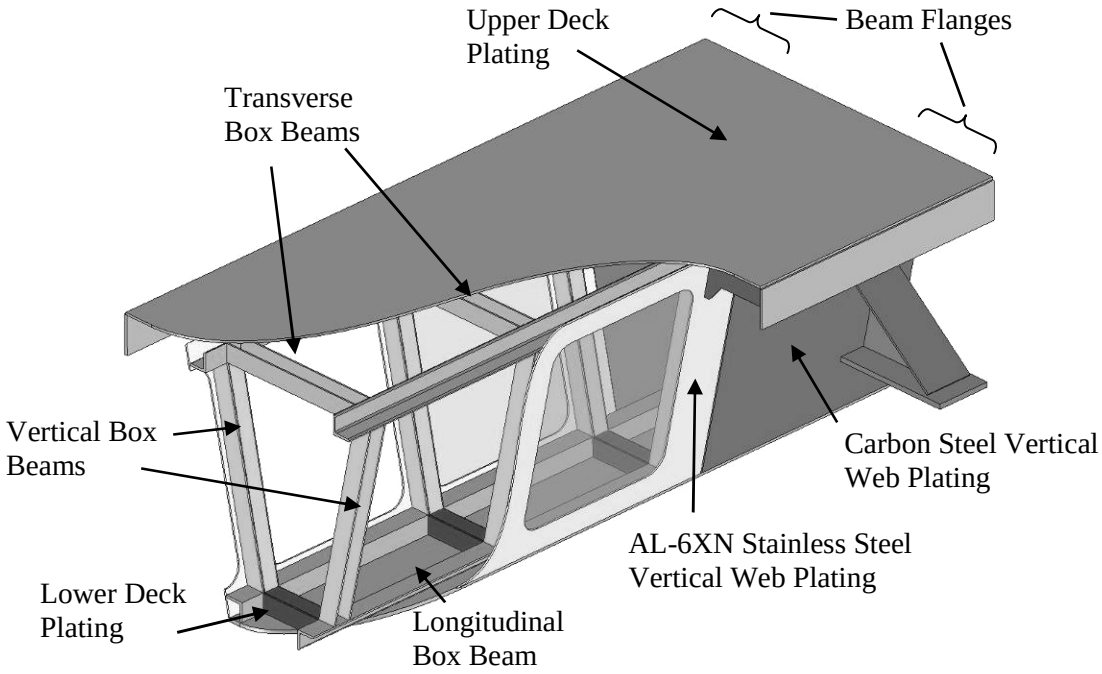


Fig. 29. Cut-away view of beam.

Loads Scaled to Represent Full Size Destoyer

The loads for the hybrid beam were based on the loads on a full size destroyer with a waterline length of 142 m and a displacement of 8300 tons. The loads on this ship, previously derived in reference [14], include the maximum slamming induced bending moment M_{sl}=2x10^9 Nm, the maximum slamming induced shear force T_{sl}=5.1x10^7 N, and the maximum bottom slamming pressure P_{bsl}=290 kPa. The present hybrid beam had a cross section approximately 1/8 the size of the destroyer, Fig. 26. The loads were therefore scaled assuming a 1:8 geometric scale in a manner which stresses the smaller model to the same level as the full-scale hull girder. Using an overhead bar for loads on the subscale model, and the linear scale 1:n, the scaled loads were

$$\overline{M} = \frac{M}{n^3} = \frac{2\times10^9\, Nm}{8^3} = 3.9 \text{ MNm} \qquad (8)$$
$$\overline{T} = \frac{T}{n^2} = \frac{5.1\times10^7\, N}{8^2} = 797 \text{ kN}$$
$$\overline{P} = P = 290 \text{ kN}$$

Note that the scaling does not represent how moments, forces and pressures scale in different size ships.

Three-Point Bending Test Design

In previous research, a six-point bending setup was used such that the maximal ABS bending moment and maximum shear force were obtained simultaneously within the beam, though at different locations [14]. This had the advantage of studying the shear and bending behavior of the structure separately (at different locations). However such loading also required a rather long specimen relative to cross-sectional height. The present specimen with a 2 meter cross sectional height was too large to allow this approach. Instead a three-point bending setup was used, as shown in Fig 30. This develops a bending moment which is greatest at the beam's center, and a shear force of constant magnitude throughout the beam with alternating sign on either side of the introduced load. The beam's span, L, was determined such that the maximum

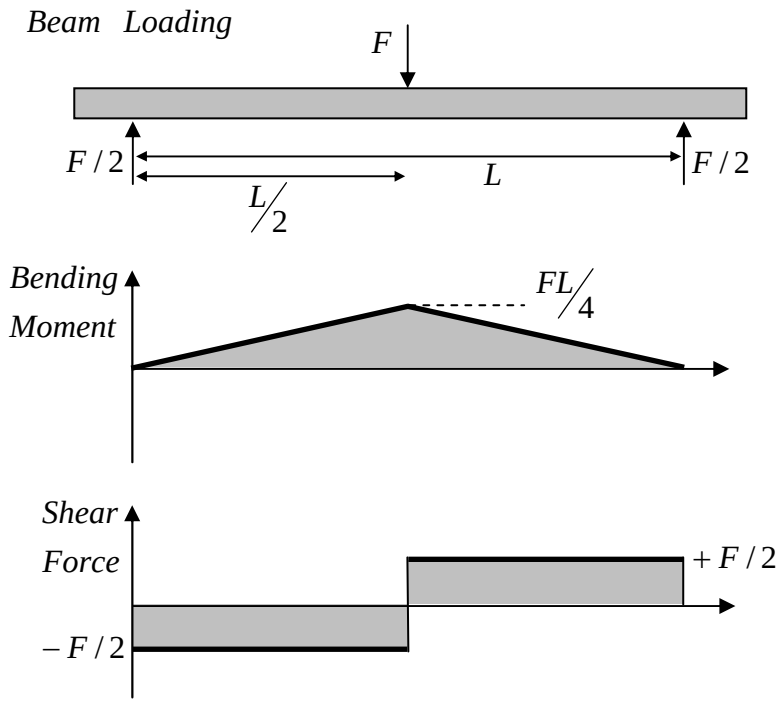


Fig. 30. Shear and bending moment for the three-point bend test

shear force $\overline{T} = F/2$ would equal the maximum shear of the scaled ship, and the maximum bending moment $\overline{M} = FL/4$ would equal the maximum scaled bending moment from the destroyer. This determined the span to be $L = 2\overline{M}/\overline{T} = 9.8\text{m}$. The beam was designed to have this length, plus and additional 0.356 m overhang at each end. The total length of the beam was thus 10.49m. The total load applied to the center of the beam was initially determined to be F = 1.6 MN.

Design of Composite Sandwich Panels

The sandwich panels were designed to carry the shear load of the hull girder without exceeding material strengths or (shear) buckling loads. Each panel was 1.59m tall and

1.34m wide measured across the opening in the steel "window" frame. Two different sandwich configurations were used. One had a plain sandwich core of uniform thickness and beveled edges, whereas the other had a core with deep corrugations facing the inside of the hybrid girder. The composite material skins facing the outside were flat in both configurations, and thicker than the inner skins. The skins were made from glass fiber reinforced vinyl ester and the cores were made of Divinycell H80 PVC based structural foam.

A preliminary design of the conventional (flat) sandwich panel was obtained by assuming that the panel carried all the shear load of the hybrid beam and that this resulted in uniform shear stress in the panels. This load can be expressed as $N_{12} = \overline{T}/(2 \cdot \textit{panel height}) = 250.6\,\text{kN/m}$ which is the shear load at the edge of each panel, per unit length. A shear strength of 200 MPa for the fiberglass skins, which is plausible for a +/-45 degree layup, requires a minimum total skin thickness (outer skin plus inner skin) of 1.25 mm. Shear buckling may be roughly estimated assuming simply supported edges, isotropic skins with E = 23 MPa, and a bending stiffness of $D = \frac{1}{2} E_{skin} d^2 t$ where d is the thickness of the core and each skin is assumed to have thickness t, and neglecting through-the-thickness shear. Timoshenko (1936) gives the critical shear buckling load to be $N_{12\,critical} = k_{xy} \pi^2 D / b^2$ where k_{xy} (equal to 8.2 for the present panels) is based upon the aspect ratio of the panels. If the skins have a total thickness 1.25mm then an H80 Divinycell core of at least 27.8mm thickness will be required to avoid shear buckling.

Beyond this preliminary analysis, a more detailed study was conducted using finite elements to determine the final panel designs. This analysis is described in more detail by Reany and Grenestedt [31]. In that paper the panels were treated as homogeneous plates with orthotropic stiffnesses. A procedure was developed for calculating the homogenous, volume average, stiffnesses of (a unit cell of) a 3D panel having a foam core, one flat skin and a second skin that could be either flat or corrugated. These homogenized plate stiffnesses were applied to a simply supported 2D plate having the dimensions of the composite panels and rotated so that all corrugations ran essentially along the compression loaded diagonal. Each plate was subjected to the shear load N_{12} described above. An eigenvalue buckling analysis was used to determine the bifurcation load for each panel design.

The final panel designs were chosen such that the conventional sandwich panel had a 44mm uniform thickness core, and the corrugated panel had a repeated corrugated pattern 150mm wide comprised of thin portions which were approximately 80mm wide and 8mm thick, and thick portions which were 70mm wide and a maximum of 66mm thick (Fig. 31). These corrugations were placed at a 50° angle to the longer side of the panel (nearly parallel to the compression diagonal) to maximize panel buckling strength. The fiberglass skins utilized Owens Corning DB240, and Hexcel 7715 fabrics vacuum infused with Ashland 8084 vinylester resin. The flat skins facing outward on the beam were nominally 1.8mm thick, while the inner skins were nominally 0.6mm

thick. The fibers of these fabrics were directed essentially along the ±45° diagonals of the panel. Further details of the panel designs can be found in Reany and Grenestedt [31].

The corrugated panels were designed to have a buckling load 25% above that of the corresponding flat panels. A knock-down factor against bifurcation buckling was incorporated against the aforementioned shear load of approximately 2.7 for the flat panel, and 3.3 for the panel with one corrugated skin. Numerical analysis predicted the resultant corrugated panel to weigh 15% less than the flat panel, in spite of its higher buckling strength. This was confirmed by weighing the finished panels. Substitution of the composite sandwich panels in place of steel web plates resulted in an overall weight reduction for the beam of 1480kg. The flat panel weighed 87% less that its steel counterpart, whereas the corrugated panel was 90% lighter than its steel counterpart.

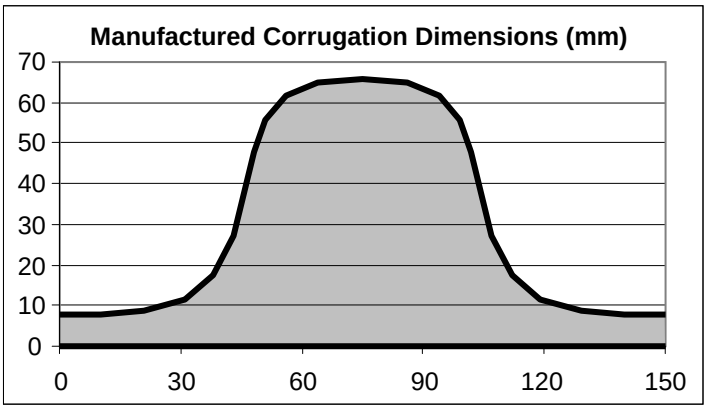


Fig. 31. Cross section of corrugation in panel that was manufactured

Preliminary Design of Steel Truss

The cross section of the all-metal ends of the large girder has a moment of inertia of

$$I_{end} = 0.1186 \text{ m}^4 \tag{9}$$

which is 9.1 times greater than the required ABS moment of inertia (scaled by a factor of $(1/8)^4$ from the full-scale ship hull). The centroid of this cross section is 1.18 m above the bottom of the beam. The maximum bending stress according to simple beam theory would be

$$\sigma = \frac{\overline{M}c}{I_{end}} = 38.9 \text{ MPa} \tag{10}$$

if subjected to the full bending moment; c (1.18 m) is the maximum distance from the neutral axis. Near the center of the beam there are four composite sandwich panels adhesively bonded to the steel truss. The moment of inertia of the steel truss is here

$$I_{middle} = 0.1091 \text{ m}^4 \tag{11}$$

and the centroid of this cross section is 1.24 m from the bottom of the beam. The maximum stress when subjected to a pure bending moment would according to simple beam theory be

$$\sigma = \frac{\overline{M}c}{I_{middle}} = 40.82 \text{ MPa} \tag{36}$$

if the contributions of the sandwich panels were neglected; here c = 1.24m. Thus replacing the steel vertical web with bonded composite panels moves the neutral axis upward by 55mm. The ABS regulations allow a maximum stress of $0.66\sigma_{yield}$ = 165 MPa (for A36 steel). This is approximately four times greater than the design stresses in the top and bottom deck, if all stress concentrations are ignored and the loading is a pure bending moment (i.e., with no shear). The girder could not carry any significant shear load with the composite panels removed.

Finite Element Analyses

Further design work on the hybrid beam structure was conducted by finite element analysis. An FE model of one quarter of the beam was constructed in Ansys 9.0 using 8-node Shell91 elements. A refined mesh was used in the highly stressed joint locations. As shown in Fig. 32 the steel windows around the composites panels were made from AL-6XN stainless steel, and given an elastic modulus of 195GPa with the FE model. The remaining portions of the beam were made from carbon steel and given an elastic modulus of 200GPa. Both steels were given a Poisson's ratio of 0.33. The composite panels were initially modeled as flat conventional, uniform thickness sandwich panels. The material properties were specified by giving the thickness of the core and skin layers, fiber orientations, and assuming generic orthotropic glass fiber properties for the skins (from Table 7). Further analysis is given below for the effects of corrugations.

Symmetry boundary conditions were used to allow this quarter-beam model to represent the entire hybrid beam under 3 point bending conditions. All nodes on the plane where $x = 0$ were constrained to have no x-displacement and no rotation about the y or z axes (referring to the coordinate system shown in Fig. 32). The nodes on the plane $y = 0$ were constrained to have no displacement in the y direction and no rotation about the x and z axes. The beam contained triangular protrusions at each end, which were intended as supports for the magnetically levitated train girder. These supports were not used for the present test. Instead vertical supports were applied under the bottom of the beam at the same x-location as the triangular supports. This was accomplished in the FE model by

constraining the z-displacement of a single node located at the edge where the bottom deck adjoins the web (and having the same x-location as the triangular support.)

A load of $F/4 = 4.0 \cdot 10^5$ N directed in the negative *z*-direction was placed on the upper deck of the quarter model of the beam at the $x = 0$ plane. FE analyses were conducted to determine an acceptable design for the introduction of the load to the upper deck (at the beam half-span location). A common method of load introduction is to position the load jacks to push on thick steel blocks which spread the load out over the specimen. Often sheets of rubber are placed between these blocks and the specimen to take up surface imperfections. Since the beam's upper deck, at the half-span location, is mainly supported from beneath by the thin walls of the vertical box beams, the concern with this loading method was that the rubber would deform locally around the location of the vertical box beams and spread the load to the unsupported sections of the deck. This could cause local bending within the upper deck which would serve to cyclically work the weld between the vertical box beam and the upper deck like a hinge. Several such configurations were modeled approximately in FE by considering uniform pressure loads on the deck over the area corresponding to load-spreading blocks. In each case significant local bending deflections were seen in the upper deck.

An alternative load introduction was designed to eliminate some of the local deformations within the upper deck. The rubber material was replaced by two 12.7 mm thick aluminum strips placed directly above the vertical walls of the box beam as shown in Fig. 33. The intention was for the aluminum to plastically deform to take up surface

imperfections in the specimen, allowing it to apply a uniform pressure over the area of each strip. These aluminum strips were loosely held in place by a retaining plate which was bolted to a thick, load-spreading steel block placed under each hydraulic load jack. The load jacks were placed in locations which would allow them to only produce in-plane loads along the vertical box beams of the large specimen (i.e. the load jack centerline and the vertical box beam centroidal axis both intersected the top of the deck). The aluminum strips were 25.4mm wide, 12.7mm thick and given differing lengths so that each produced the same average pressure on the beam. The inner strips were 162mm long and the outer strips were 300mm long, with both producing a pressure on the deck of 68 MPa at the design load 2P. Ultrasonic measurements were used to locate the vertical box beam walls beneath the deck. Further details of the loading used during the test can be found in Reany and Grenestedt 2008 [31].

The load introduction was simulated in the FE model by placing the load as a uniform pressure over two areas corresponding in size to the aluminum strips. The resulting deflections in the deck panel were greatly reduced (in comparison with the standard loading method), with maximum deck von Mises stress being below 150 MPa (see Fig. 34).

The FE model was used to predict both local and global behavior of the beam. At the design load the deflection at the center of the deck of the beam (at the beam half-span) was 11.1 mm. Fig. 35 depicts a side view of the beam with deformations scaled up 20

times for visibility. An outline of the undeformed beam overlays the deformed model. From this picture it is clear that

Table 7. Material Properties.

Material Property	Hexcel 7715	Owens Corning DB240
Ex	31.3 GPa	23 GPa
Ey	12.8 GPa	20 GPa
Ez	12.8 GPa	100 Mpa
Gxy	4.1 GPa	10.0 Gpa
Gxz	4.1 GPa	7.1 GPa
Gyz	1.5 Gpa	7.1GPa
νxy	0.30	0.275
νxz	0.30	0.275
νyz	0.39	0.275

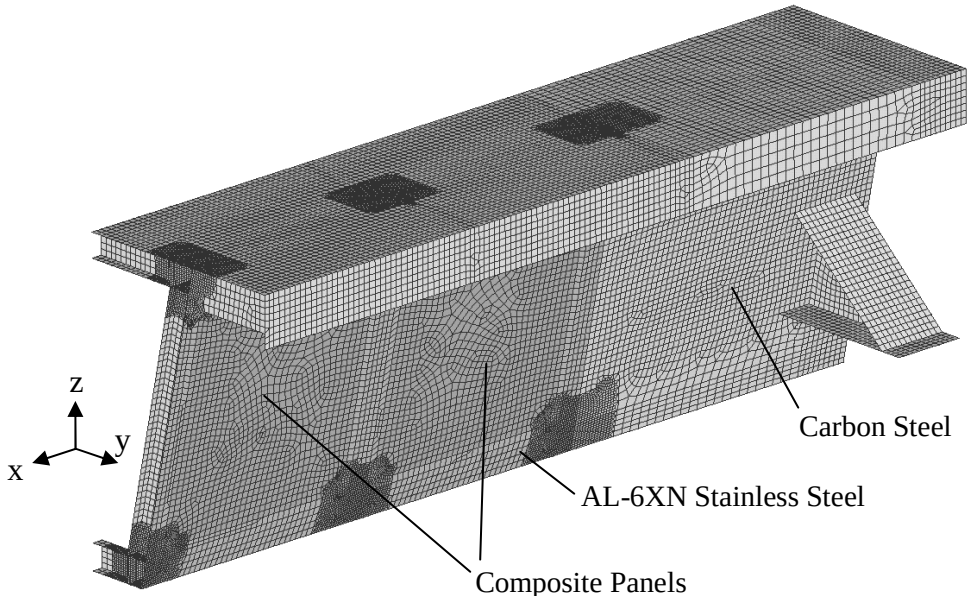


Fig. 32. FE model of one quarter of the large hybrid beam.

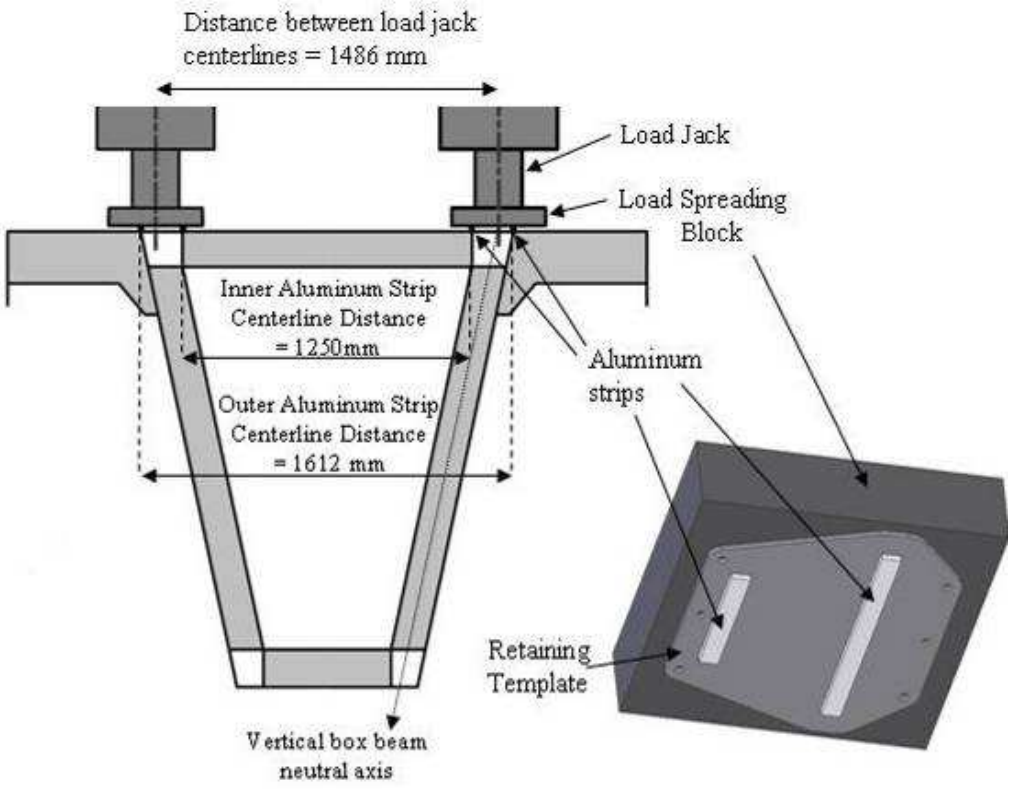


Fig. 33. Load introduction setup.

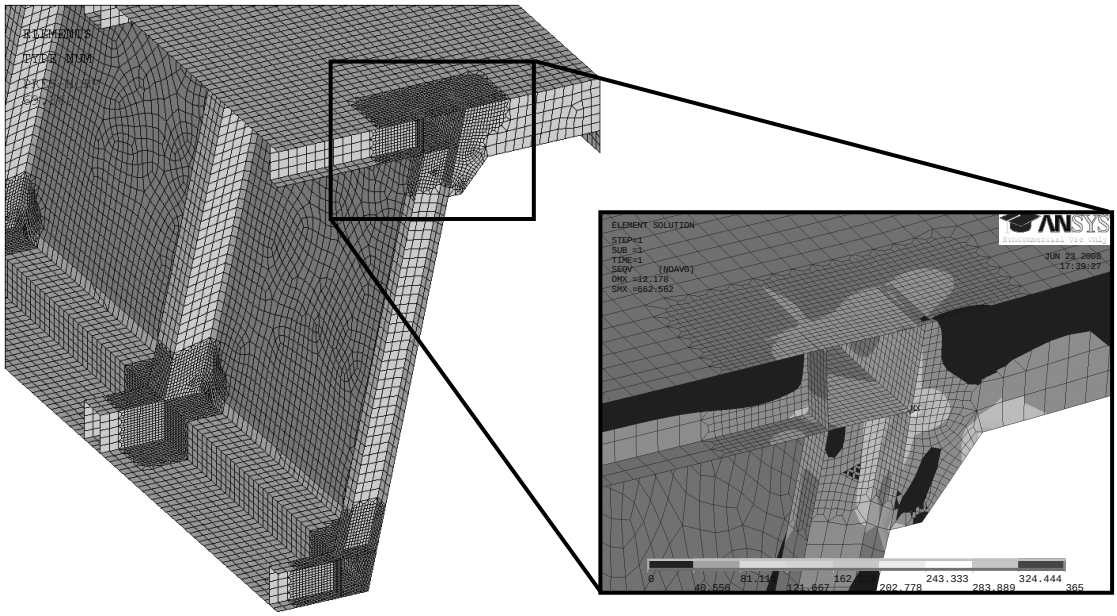


Fig. 34. Von Mises stress near load introduction.

Loaded center of beam
(symmetry plane)

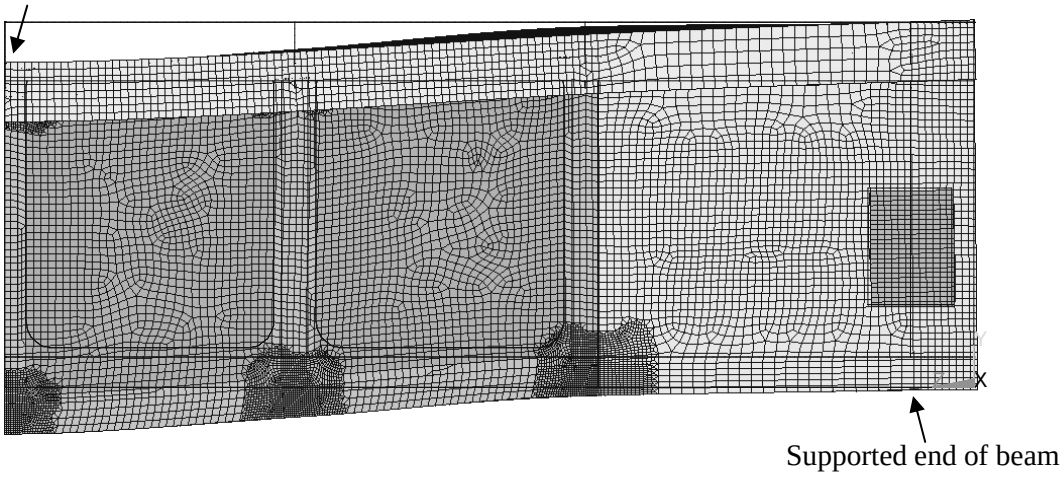


Fig. 35. Side view of deformed quarter-beam FE model.

the composite panel sections of the beam are more compliant than the sections which use steel webs.

High stresses are produced in the steel near the corners of the composite panels. Among these corners, those which are located at the transition between the all-steel sections and the composite paneled sections have the highest stresses. This is believed to be due to the difference in the stiffness of these sections, and the associated localized deformation. The corner highlighted in Fig. 36 contains the highest of such stresses. The corner radius in the steel was chosen to be 150mm which brings the maximum von Mises stress in the steel to 350MPa or 96% of the material's yield stress (at design load).

As mentioned earlier two special panels were used on the beam, having deeply corrugated inner skins oriented essentially parallel to the compression diagonal of the panels. These two panels were paired up across the beam from each other (so as to not induce beam-twisting under load), and towards one end of the beam. The FE model was used to investigate the effect that these panels would have on the beam. Effective plate stiffnesses for the corrugated panel were generated using the analysis technique presented in [31], and the reference plane about which the $B_{\alpha\beta\gamma\delta}$ and $D_{\alpha\beta\gamma\delta}$ stiffnesses were calculated was taken to be at the flat outer skin of the panel (see Table 8 for detailed stiffness listing). These stiffnesses allowed flat 2D shell elements on the large beam model to represent the complicated corrugation pattern. To apply these properties to the beam, 4-node Shell 181 elements had to be used for the entire FE model (as these are the only Ansys elements that support the use of the available plate stiffnesses). Both

the transition from 8-node to 4-node elements, and the addition of the corrugated panel were determined to have little effect on the global deflections and stresses within the structure. However, the corrugated panel exhibited a marked out-of-plane deflection (panting) effect, while the flat panels did not. This can be seen in Fig. 37 which shows the quarter beam model with both a flat and a corrugated panel. The out-of-plane deflection of the corrugated panel was almost an order of magnitude greater than that of the flat panel.

The reason for the panting effect can be explained as follows. Both flat and corrugated panels are placed under a shear loading introduced in the plane of the flat outer skin. This leads to one diagonal of the panel being loaded in compression, and the other in tension. Since the coupling

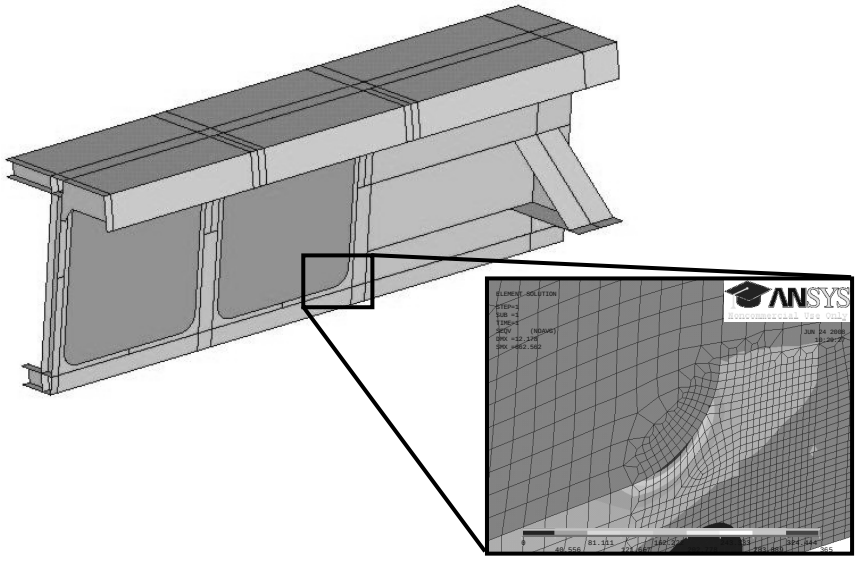


Fig. 36. Panel corner von Mises stress.

Table 8. Plate Stiffnesses for Corrugated Panel

Material Property	Corrugated Panel
A1111	7.77E+07
A2222	4.71E+07
A1122	1.30E+07
A1212	2.23E+07
A1112	4.01E+01
A1222	5.67E+01
B1111	9.32E+05
B2222	3.35E+04
B1122	1.00E+04
B1212	5.76E+04
B1112	1.48E+00
B1222	-3.52E-01
D1111	4.39E+04
D2222	4.40E+02
D1122	1.32E+02
D1212	1.91E+03
D1112	1.13E-01
D1222	-2.20E-03
E11	4.18E+06
E22	3.24E+05

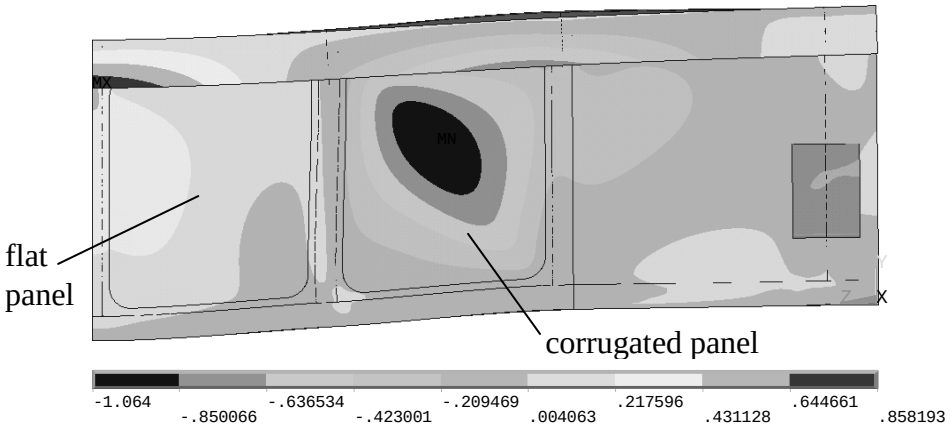


Fig. 37. Out-of-plane deflection of corrugated and conventional composite panels within the large hybrid beam.

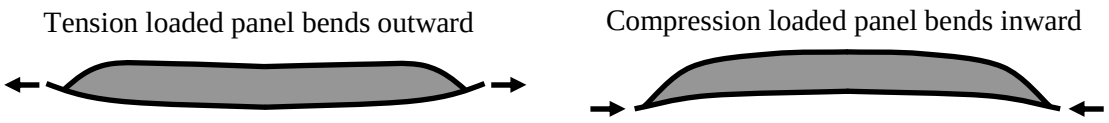


Fig. 38. Schematic of deformed tension and compression loaded panel 2D cross sections.

stiffnesses of the panels are non-zero, the in-plane loading introduces out-of-plane deflections as in the 2D panel cross sections shown in Fig. 38. For the flat panel, the tension loaded diagonal wants to bend outward on the beam, while the compression loaded diagonal wants to bend inward. These two effects tend to cancel each other out, leading to small net out-of-plane deflections for these panels. However, for the corrugated panels, these effects do not cancel each other and a relatively large net inward bending deformation results.

Fatigue Life Estimate of the Steel Truss

Fatigue is a major issue of welded steel and fairly detailed finite element analyses were performed to estimate the fatigue life of the steel structure. The steel truss contained a number of details that have fatigue issues. These can be categorized into different "fatigue categories" frequently used in civil engineering. Each category (denoted A, B, B´, C, D, E and E´) is distinguished by the joint geometry, with the severity of fatigue problems being ranked from A to E´ where E´ is the worst. Ref. [36] gives many examples of typical joint geometries for each category, and establishes S-N curves for

each. These S-N curves are reproduced here as Fig. 40. The following paragraphs cover the fatigue details of interest on the steel truss, in order of increasing severity. Refer to Fig. 28 for beam terminology.

For the steel frame, all the longitudinal fillet welds between the flanges (top and bottom) and the web plates are governed by Category B. However, judged by the appearance of these welds, the fatigue strength may be a bit less than that of Cat. B (e.g. Cat. B'). Similarly, all the longitudinal welds which connect the L-shaped steel bars to the deck and webs (to form the longitudinal box beams) are of Cat. B or slightly lower in strength. The butt welds at the end of the AL-6XN box (connecting the AL-6XN web plate to the carbon steel web plate) are also Cat. B. The highest stress levels near any of these fatigue details are found at the location shown in Fig. 39 where the L-shaped angle of the longitudinal box beam is welded to the web (near the transition between the compliant composite webs and the stiff steel webs). Von Mises stress levels in the region surrounding this fatigue detail are shown in Fig. 39. There is not a high stress gradient seen near the weld, thus it seems plausible to take the nominal stress level to be the highest stress level seen in this area (approximately 140MPa). This nominal stress is then used with the S-N curves found in Fig. 40, to estimate fatigue life. This indicates that such welds could survive more than 10^6 cycles at this load. Thus all Cat. B details were deemed to be not critical.

The transverse welds between the vertical box beams and longitudinal box beams are placed in fatigue Category C. FEA estimates the highest nominal stress near a

transverse weld to be approximately 130 MPa for the design loading. Fig. 40 indicates that such welds could survive approximately 10^6 cycles at this load. Thus these details were also deemed to be not critical.

The corners formed at the intersections of the transverse and longitudinal box tubes are Cat. E details. These are the most serious details in the steel frame, the worst of which is shown in Fig. 39. Finite element analysis shows a strong stress gradient near to this detail, thus it is not immediately clear what stress to use for comparison with the SN curves. Typically a stress is used with the fatigue data which is derived from simple hand calculations, giving the nominal or "far-field" stress within the member. Such hand-calculated stresses neglect the stress rise near the singularity. However, hand calculations are not practical for the present, complicated structure. Instead, a secondary finite element model was used to establish a relationship between stresses seen in finite element models near to the corner and an idealized "far-field" stress away from the singularity. This secondary model consisted of a metal strip in tension with a perpendicular welded tab at its center. This strip was given materials and dimensions consistent with the box beams on the hybrid structure. The stress 10 mm out from corner of the welded tab was then observed to be 10% higher than the nominal stress within the strip (Fig. 41). Thus it was assumed that the same relationship holds within the hybrid beam.

The stress near the Cat. E. detail in Fig. 39 is shown below in refined detail in Fig. 42. At a location 10 mm out from the corner the stress is approximately 170 MPa.

Following the example of the strip with the welded tab, this could be expected to be approximately 10% higher than the far-field stress within the member. Thus, the far-field stress which was chosen to be used for comparison with the Cat. E curves of the SN graphs was 155 MPa. This suggests a fatigue life for these details of less than 10^5 cycles. For this reason it was decided to lower the maximum cyclic testing load to 70% of the design load (to 11.16×10^5N). At this lowered level the far field stress should be 0.7×155MPa or 109MPa, resulting in a fatigue life of between 1×10^5 cycles and 3×10^5 cycles, depending on whether this is considered an E or E' detail.

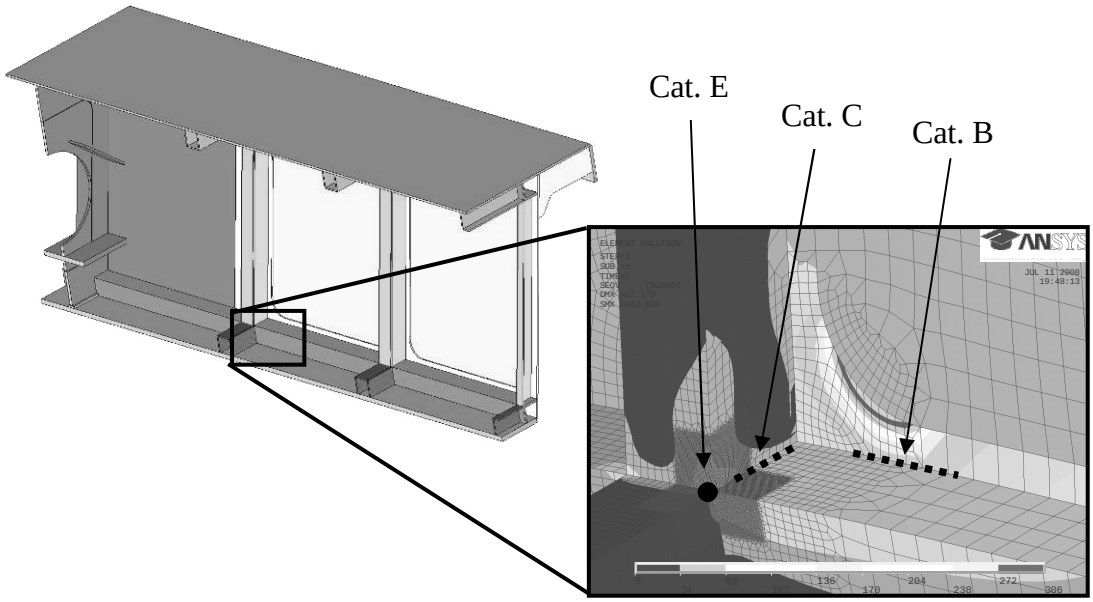


Fig. 39. Von Mises stress near the worst category B, C and E fatigue details.

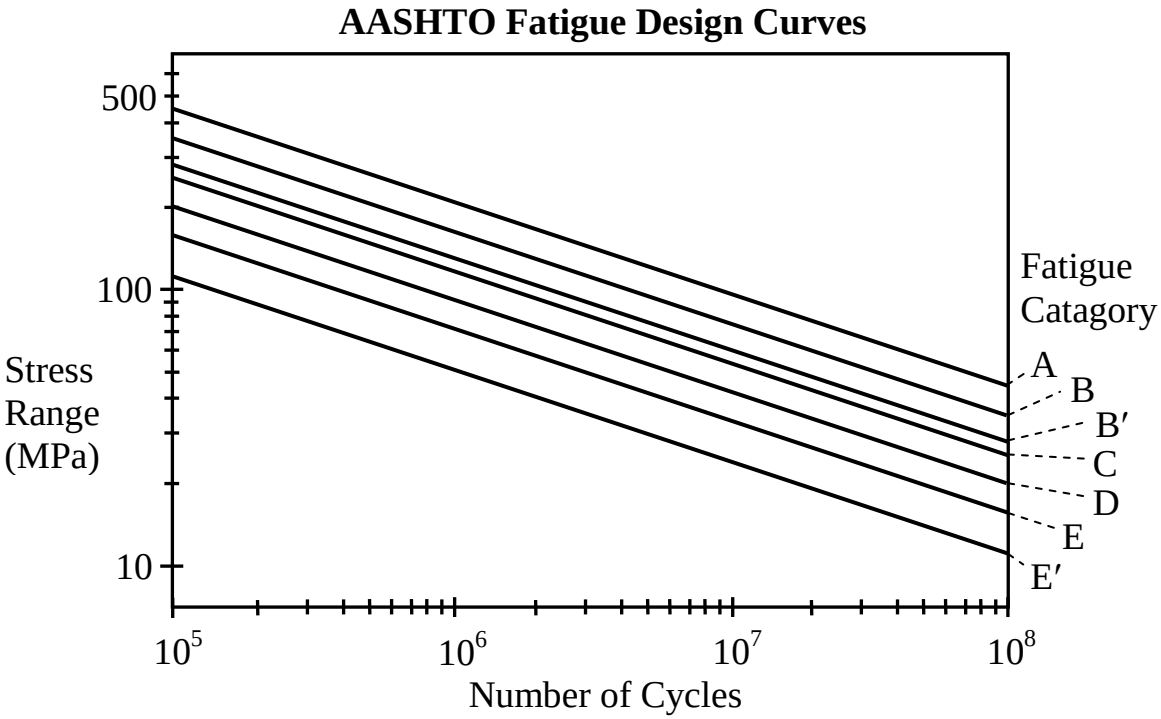


Fig. 40 . S-N curves for fatigue categories

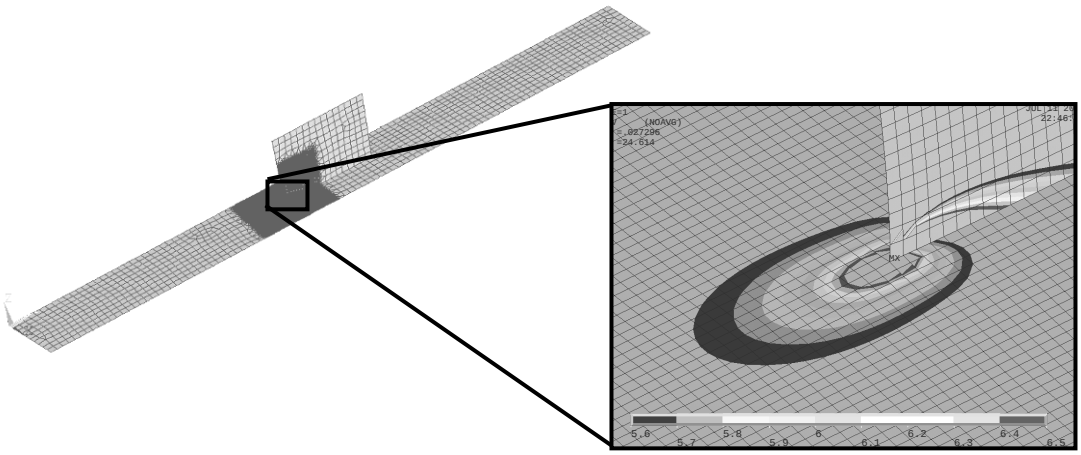


Fig. 41. Secondary FE model used to predict “far-field” stress near singularity.

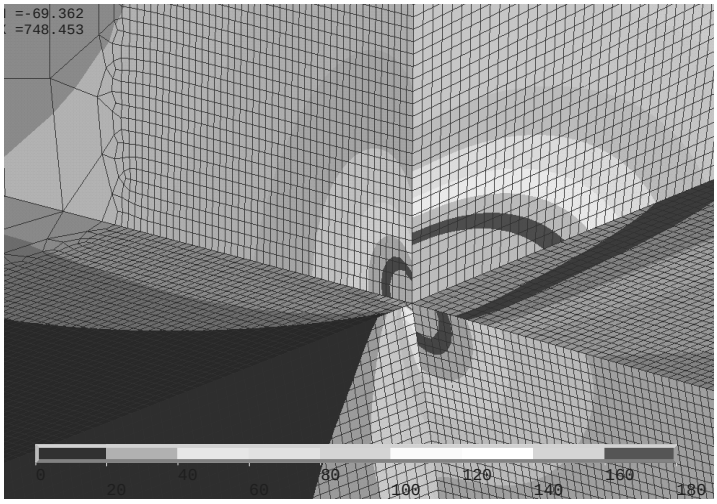


Fig. 42. Refined von Mises stress levels near to the Cat. E detail.

Steel Manufacturing

The steel structure was manufactured by Maglev Inc. (McKeesport, PA, USA). The completed steel part of the hybrid beam was then shipped to Lehigh University for outfitting and mechanical testing.

Composite Sandwich Panel Manufacturing

As was previously mentioned, a description of the design of the composite sandwich panels has already been published in Ref. [31]. For the present hybrid truss, six panels were manufactured with conventional flat fiberglass skins on both sides. The remaining two panels were given one flat outer skin and one deeply corrugated inner skin. The panels were made by 5-axis CNC routing of foam cores, and vacuum infusion of the glass fiber skins onto the cores.

The core of each sandwich panel was made from Dinvinycell H80 structural foam. These cores were given dimensions 1.54m x 1.29m with a 125mm corner radius, which is 25mm smaller all around than the corresponding windows in the steel frame. The conventional panels had flat cores machined to 44mm thickness. The side of the panel to face inward when installed on the beam was given a 45° bevel around the border, with a 100mm radius fillet added to soften the edge of the bevel. This bevel allowed the fiberglass skins on either side of the core to come together at the panel edge to form a thin flange which was used for bonding to the steel beam. Extra fabric layers were

added on the beveled portions of the core, and also between outer and inner skins around the panel edges to thicken the bonding flange. Infusion grooves 2mm wide and 2mm deep were machined into the core in two perpendicular directions. These grooves were spaced apart by 25.4mm and matching through-holes were drilled connecting the infusion channels on both sides of the core. Corrugations were tapered and rounded off at the panel edges to allow the fiberglass fabric to lay nicely, and to allow the outer and inner skins to come together to form a bonding flange around the panel. The cores of the corrugated panels were CNC routed with a large ball end mill in sweeps parallel to the corrugations. Subsequently infusion grooves and through holes, having the pattern mentioned above, were machined. A corrugated and a conventional core are shown in Fig. 43 and Fig. 44. To make each panel core, multiple sheets of foam were bonded together using 3M Scotch-Weld DP125 epoxy. Hourglass foam shapes, such as the one visible in Fig. 44, were used as keys for joining and aligning the foam cores.

The fiberglass skins were made by vacuum infusing Owens Corning DB240, and Hexcel 7715 fabrics with Ashland 8084 vinyl ester resin onto the cores. This process took place on a large laser-leveled aluminum table, with the skins facing outward on the hybrid beam placed down against the table, and the beveled skins facing upward. Each infusion took place in under 2 hours, and panels were left under vacuum on the table for at least 24 hours. After de-molding each panel was allowed to cure at room temperature and pressure for several months. At this point the panels were trimmed to size, leaving a 125mm unsupported (skins-alone) flange around the border of the foam core.

Panel Bonding to Steel Structure

Investigations were made to determine an appropriate bonding overlap between the composite panel flange and the steel window. Single lap shear tensile tests were conducted on 16 specimens constructed from fiberglass, bonded to 9.5mm thick AL-6XN stainless steel using Henkel E2119 epoxy adhesive. The fiberglass portion of the specimens consisted of 14 layers of Owens Corning WR24-5×4 (0º/90º) fabric infused with Ashland 8084 vinyl ester resin, resulting in a thickness of approximately 9 mm. Four of the specimens were made with the glass fibers in the ±45° direction, and twelve were made with the fibers in the 0º/90º direction. The specimens were 100 mm wide. Eight specimens were made with a 50 mm overlap and another eight with an 80 mm overlap. The bond area of the stainless steel was grit-blasted and cleaned with trichloroethylene. The bond line thickness was controlled by embedding a 0.8mm wire between the bonded surfaces. These single lap shear specimens were tested to failure in a mechanical test frame. The resulting shear failure stresses ranged between 8.6 MPa and 17.9 MPa, with the average for the ±45° specimens being 11.4 MPa and the average for the 0º/90º specimens being 14.1MPa.

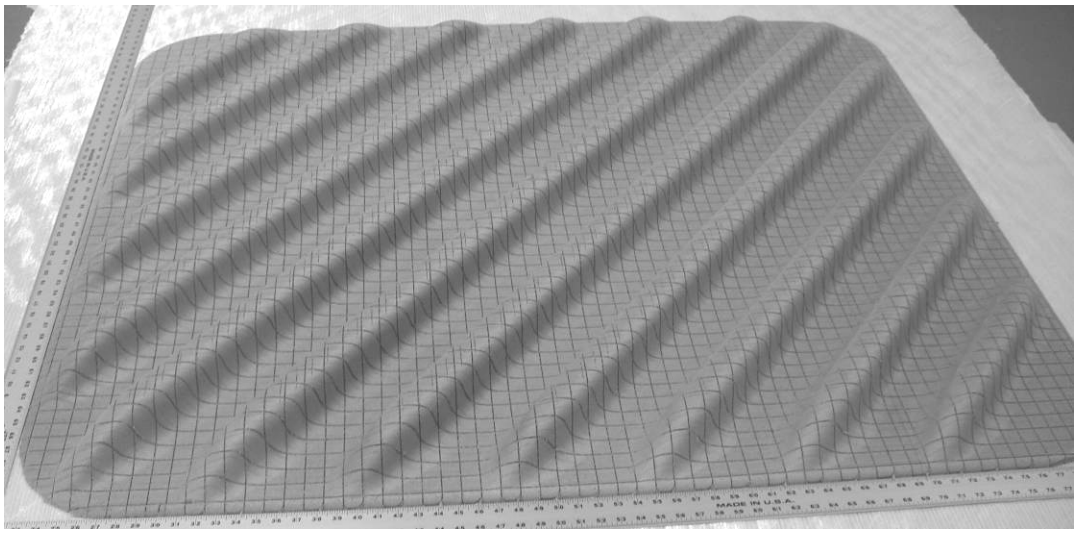


Fig. 43. Machined foam core for a corrugated skin sandwich panel.

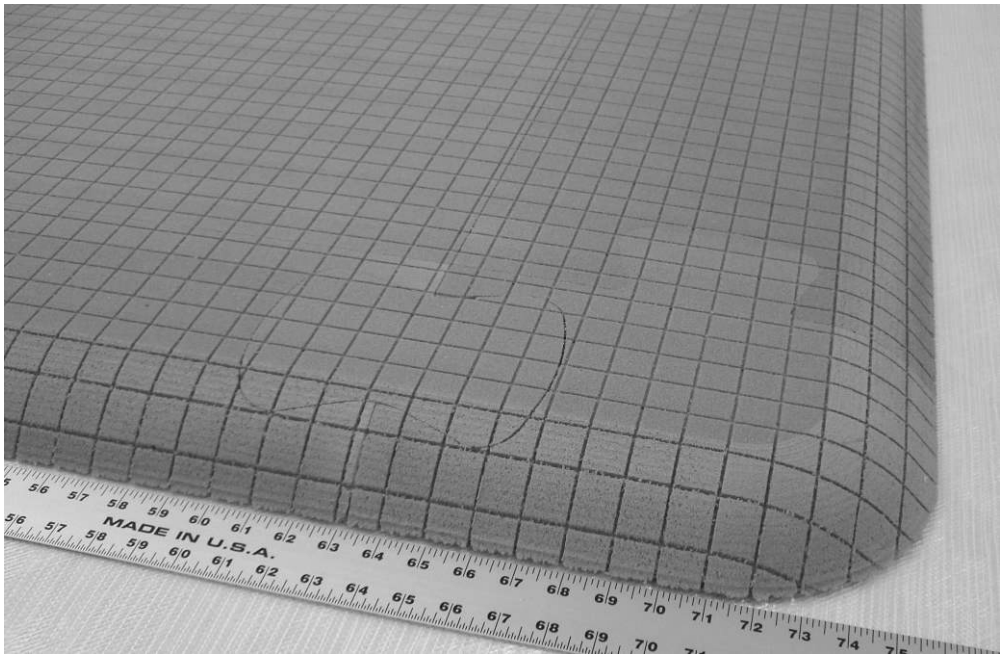


Fig. 44. Machined foam core for a conventional sandwich panel.

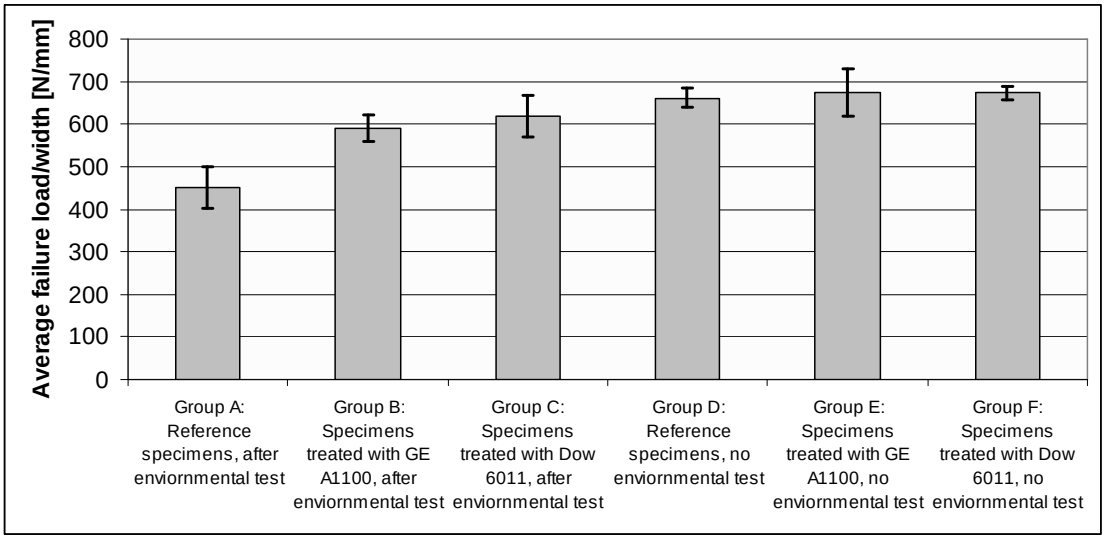


Fig. 45. Results from single lap shear testing with untreated and Silane treated steel adherends.



Fig. 46. Aluminum fixture used for adhesive bonding of composite panels to steel structure.

Assuming that the vertical shear P in the hybrid girder is carried completely by the composite panels, each individual panel would carry an average shear loading of N_{12} = $2.5 \cdot 10^5$ N/m along each edge of the panel. A bonding overlap of 100 mm would then result in an average shear stress (in the adhesive joint) of 2.5 MPa, which appeared feasible for the fatigue loaded hybrid beam specimen.

Tests were also conducted to determine the effect of a Silane adhesive promoter. Twenty-four lap shear test specimens were constructed from fiberglass and 2.7 mm thick AL-6XN stainless steel. The fiberglass portion of the specimens consisted of 5 layers of Owens Corning WR24-5×4 (0º/90º) fabric infused with Ashland 8084 vinyl ester resin, resulting in a thickness of approximately 3.2 mm. The width of each specimen was 25.4 mm and the bond overlap was 50 mm. Again Henkel E2119 was used for the bond, and the metal was grit-blasted and cleaned with trichloroethylene prior to silane treatment. The specimens were arranged into three groups of eight. For one group, the stainless steel was treated with Dow Silane 6011 prior to bonding. This was simply wiped onto the metal and allowed to dry. The second group was given a similar treatment of GE A1100 Silane. The third group was used as a control and given no adhesive promoter. From each group of eight specimens, four were tested immediately and four were given a week-long environmental cycling prior to testing. Each 2 hour cycle consisted of the temperature being altered between -20ºC and +80ºC, at a constant relative humidity (RH) of 80%. The results are shown in Fig. 45. The specimens which were tested without prior environmental cycling had little difference

between their failure loads. However, after environmental cycling, the specimens which had a Silane treatment had favorably higher failure loads.

A bonding overlap of 100mm length was used for attaching the panels to the hybrid girder. In preparation for the bonding, the steel of the beam was sanded with a 40 grit grinding wheel, and cleaned with trichloroethylene. Dow Silane 6011 was wiped onto the beam one hour prior to bonding. Henkel E2119 epoxy adhesive was used for bonding with approximately 0.1% by volume 0.18mm max diameter glass beads to control bond thickness. This adhesive was applied by using six pneumatic adhesive guns and static mixing tubes. An aluminum rig was constructed to facilitate moving the panel throughout the bonding process (see Fig. 46). The panel was attached to the rig temporarily through the use of four vacuum suction cups. The rig was clamped to the metal structure of the beam and it allowed the panel to swing up to the window opening of the beam, as well as swing away from the beam for adhesive application. During bonding adhesive was applied to the panel flange, and the panel was swung into location on the hybrid beam. The aluminum rig was then ratchet-strapped to the steel beam to hold everything in place. An inflatable rubber bladder backing the flange of the panel, and located within a U-channel section of the aluminum rig was used to apply generous pressure to the flange of the panel. This insured a good bond clamping which was applied for at least 12 hours. After this the aluminum rig was removed, and excess adhesive trimmed from the panel edges.

Chapter 4

GFRP SANDWICH TENSILE TESTS WITH EMEDDED STRAIN GAGES

The strains on the outer skin of a composite sandwich panel on a boat bottom needed to be measured but foil strain gages could not be attached to the outer skin using traditional methods because they would soon be damaged and the wires would be unacceptable. Different methods for measuring strain in the lab and in the field are discussed in Shukla 2004 [37]. From Shukla as well as Guemes [38] an applicable method for measuring strain inside of a panel would be embedded optical gages. At present the strains needed to be measured accurately, cost effectively, and the test setup needed to be able to withstand harsh conditions. The leads of embedded optical gages exiting from inside sandwich panels are fragile, and the gages need expensive equipment to run which may not work inside a boat in rough seas. This chapter addresses the fabrication and testing of glass fiber reinforced plastic (GFRP) sandwich panels with embedded foil strain gages.

Embedding Strain Gages

The first task was to embed strain gages in a vacuum infused sandwich panel. The sandwich panel would consist of two GFRP face sheets on either side of a closed cell PVC foam core. The surface of the PVC foam core was too porous to attach strain gages to. In order to overcome the roughness of the foam core surface, the strain gages

were bonded to flat thin fiberglass plates that would not noticeably affect the strength of the panel nor the readings of the strain gages. These fiberglass plates were made of a single layer of Hexcel 7725 glass fiber fabric infused with Ashland 8084 vinyl ester, cured at room temperature, and cut into shapes suitable for the strain gages. Paddle-like shapes were cut using an abrasive waterjet cutter, Fig. 47. These 50.8mm diameter paddles have a flat area for the strain gage to be bonded to, holes around the perimeter that act as a stiffness gradient, and a 'handle' to bond the leads of the strain gage to. These paddles with strain gages were then bonded to the foam cores.

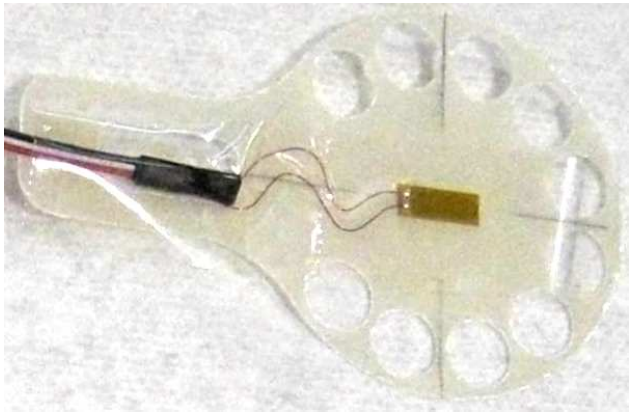


Fig. 47. Strain gage with strain relief bonded to FRP paddle.

Vishay C2A-13-250LW-350 leaded strain gages were bonded to the GFRP paddles using Vishay's M-bond AE-10 two part general purpose epoxy and following the instruction bulletin for bonding strain gages [24]. The AE-10 epoxy over the strain gage was cured at room temperature for 24 hours. The sandwich panels in which the strain gages were to be embedded were expected to experience high strains. An attempt to protect the leads from breaking under high strains was made by attaching the leads with

two-part high elongation epoxy in a zigzag pattern to the paddle to give some strain relief, Fig. 47. The adhesive DP-125 from 3M was used for its 130% elongation properties to hold the lead wires in the zigzag pattern.

Electric wires are needed to connect the strain gages with the data acquisition system. To accommodate the wires, 6.4mm wide channels were machined in the foam core from the strain gages to the corner of the panel, Fig. 48. These channels were at a depth near the neutral axis of the sandwich panel, thus reducing strain in the electric wires as the panels deform (in bending). After the channels were routed, the foam core was flipped over, indexed, and routed to a similar geometry (thickness, taper, infusion grooves) as a typical boat panel for the slamming test rig [40].

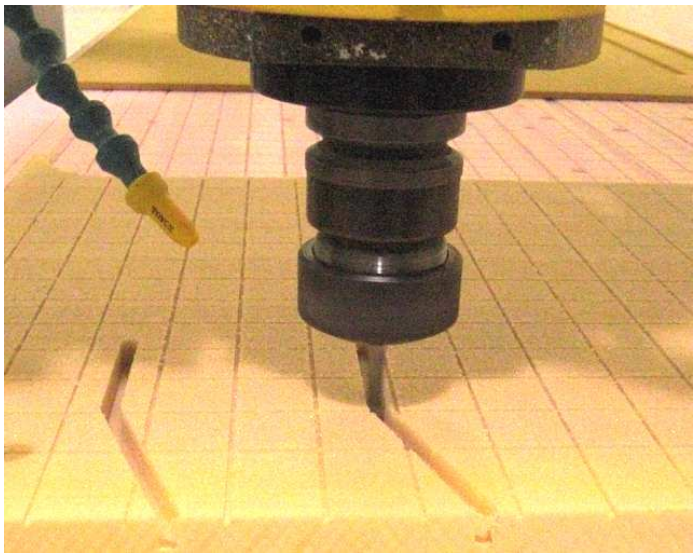
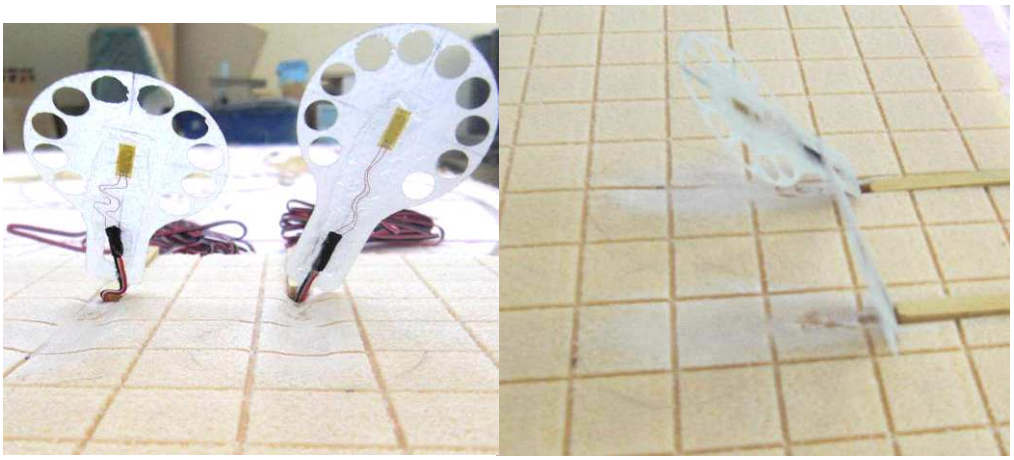


Fig. 48. Machining channels into foam core for strain gage wires.



a) b)

Fig. 49. Strain gage paddles prepared to be bonded to PVC foam core.

The paddles were not completely flat due to the wires and epoxy and in order for the paddles to lie flat on the cores some foam was removed by sanding a depression with 80 grit sandpaper. Fig. 49 shows the paddles ready to be bonded to the foam core with the depression in the foam core made so they would lay flat. The paddles were aligned and bonded in place using 3M's DP 125 two part epoxy and clamped using a flat board with a heavy weight for at least six hours. A bonded paddle with strain gage is shown in Fig.50.



Fig. 50 Paddle epoxied flush to the foam core

In order to hold the wires in place as well as fill-in the channel where the wires were placed, filler pieces were CNC routed out of the same H250 foam as the core. Once the paddles were bonded, wires were positioned in each channel. In order to protect the wires, they were passed through silicone tubing, which was wedged in between the neutral axis of the foam core and the foam filler pieces. Once all the wires were positioned correctly, the wires, channels, and silicon tubing were bonded to the core using 3M's DP125 with the wires running out of the corner of the core, Figs. 51-53.

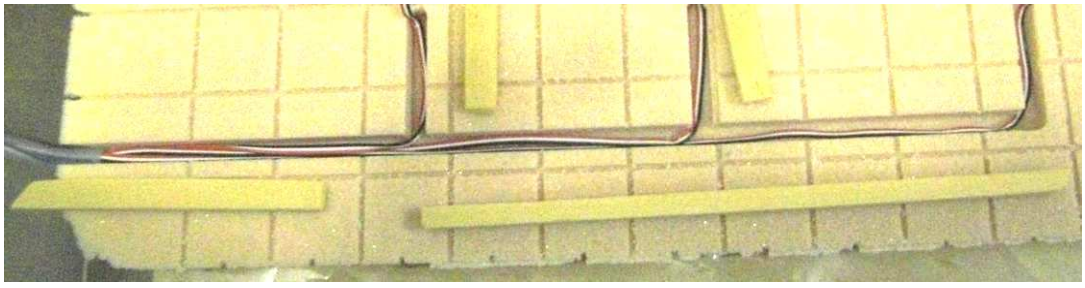


Fig. 51. Wires routed through the channels to the edge of the foam core and through the protective tubing.

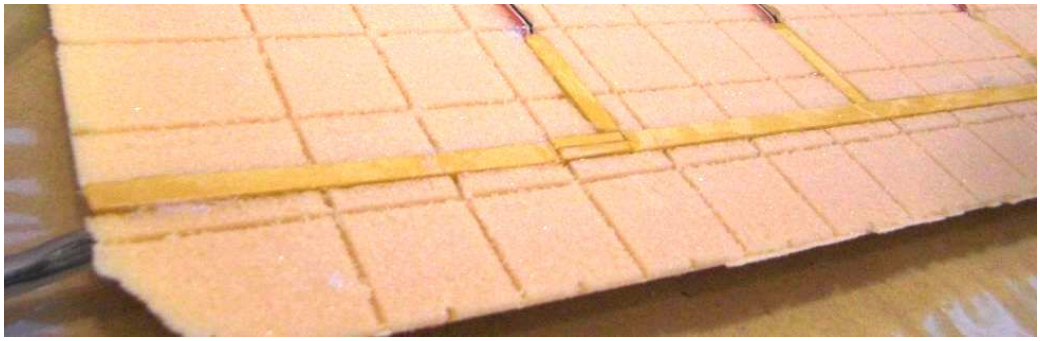


Fig. 52. Filler tabs bonded to the foam core with the lead wires exiting the foam core.



Fig. 53. Strain gage wires exiting foam core through protective tubing

Panel Manufacture

The foam cores of the of the sandwich test panels were routed out of H250 PVC foam to a similar geometry as the designed panels for the high speed boat previously mentioned. The test cores were both routed flat to 18mm thickness, with a corner radius of 50mm, bevel of 30 degrees, 50mm fillet to blend the bevel, 2x2mm infusion grooves spaced 25.4mm apart, and 6.4mm wide channels for running strain gage wires. The only

differences between the test panels and the panels for the high speed boat were their length and width. The size of the core for the test panel was 355x254mm.

The design of the panel was for 1.98mm outer skins and 1.32mm inner skins. Using Owens corning DB240, a stitched +/- 45 degree glass fiber fabric, gave the layup three layers on the outside and two layers on the inside. To transfer the load from the single skin flange, two layers were used as reinforcement layers extending 25 and 45 mm past the fillet.

The test panel was laid up with the three layers for the outer skin on the table, followed by the core with the embedded strain gages followed by the two inside layers and two reinforcement layers. The four layers of fabric on top of the wires coming out of the core were carefully lifted and supported around the wires. Tweezers were used to carefully move the tows of each layer out of the way to locally make a hole to pass the wires through. The tweezers pulled the ends of the wires through the fabric which was lifted off the table slightly so the wires would not pull on any strands of fiberglass while being pulled out. The wires were pulled until the silicone tubing was fully out. The four layers were then carefully placed back into position, Fig. 54. The wires were then passed through a small hole cut into a piece of peel ply that covered the entire layup.

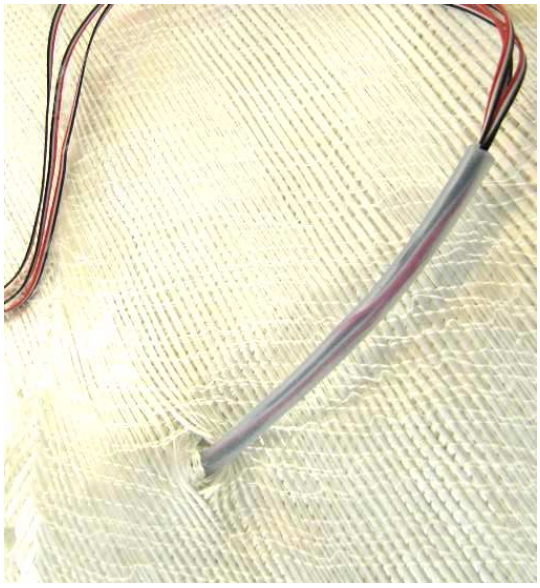


Fig. 54. Wires pulled through the top fiberglass layers

To protect the wires from being covered with resin, the wires were enclosed in a piece of vacuum bag with vacuum sealant tape. Pieces of breather were placed under the tube and the wires enclosed in vacuum bag, to try and limit any indentation in the finished panel. The entire layup was covered with vacuum bag, sealed with vacuum sealant tape, and evacuated of air, Fig. 55.



Fig. 55. Panel and encased wires covered with vacuum bag

The panel was vacuum infused with Ashland 8084 vinyl ester resin and left under vacuum to cure at room temperature for 24 hours before demolding. The panel was successfully infused without any problems. The tubes and wires showed no damage and no marks were visible on the finished panel where they were vacuumed down, Fig. 56.

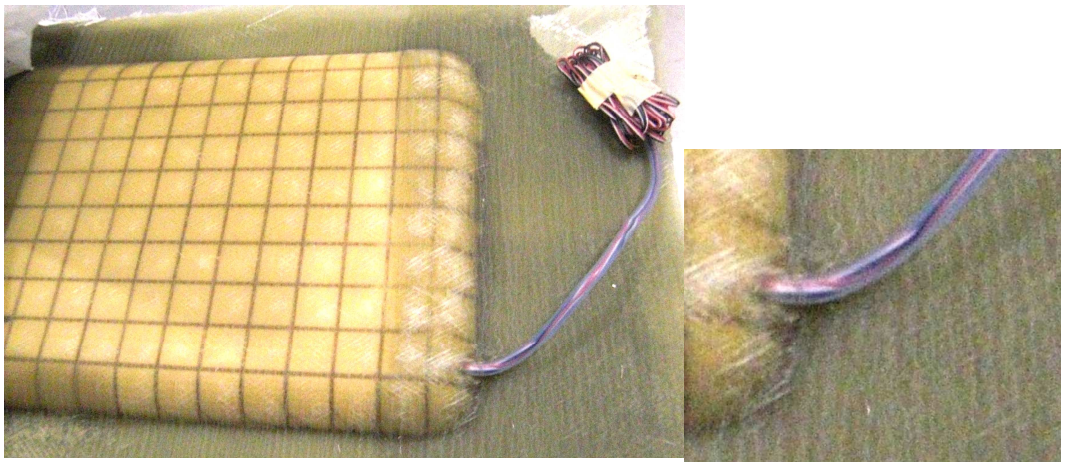


Fig. 56. Demolded test panel with detail of wires exiting core.

Comparing readings of embedded and external strain gages

A second sandwich panel was made with embedded strain gages to test the accuracy of having strain gages on the inside of the skin next to the core of a sandwich panel. The panel was cut into specimens to be tensile tested and the results compared to the traditional method of the strain gages attached to the outside of the skin.

The layup of this second test panel was similar to the previously described panel but had several differences. The tensile test specimens would be loaded via pins through clevases in the test machine. The edges of the sandwich panel were therefore reinforced for the pin loading. A solid piece of GFRP was butt joint to the core and the skins were infused on top and bottom.

The same flat 18mm thick, H250 foam core previously described was used and channels were routed for the wires to run along the neutral axis. The channels ran from the strain gage paddle, down the center line, and then veered to one side to prevent the wires from being damaged when cutting the hole for the loading pin. The routed core was bonded to a solid piece of GFRP slightly thinner than the foam core. The strain gage paddles were bonded to the core and the wires ran through the channels, up to the surface and straight back to the edge of the solid GFRP piece. Care was taken to epoxy the wires in place over the solid GFRP. If the wires were not straight; they risked damage when the tensile specimen was cut, Fig. 57.

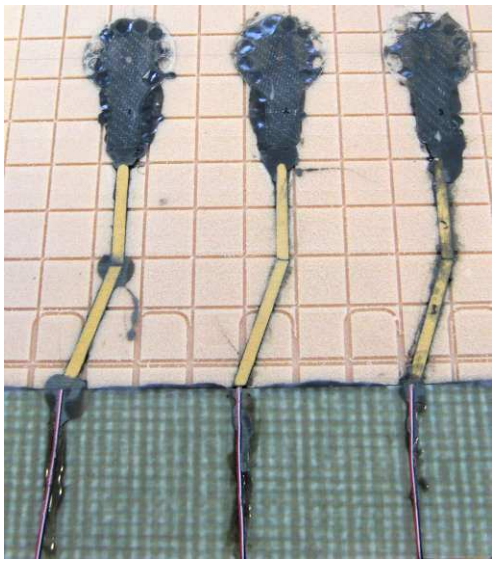


Fig. 57. Strain gage paddles bonded in place with wires routed through the core and over the solid GFRP piece

The sandwich was layed up on a laser leveled large aluminum infusion table. Glass fiber continuous filament mat was used over the solid GFRP piece to aid infusion.

Three layers of DB 240 reinforcement with +/- 45° glass fiber, where the 0°direction is along the specimen and parallel to strain gages, were placed on the aluminum table followed by the foam core/solid GFRP piece, and three layers of DB 240 +/- 45° glass fiber. The wires were covered with peel ply, then sealed in a vacuum bag "pouch" with vacuum sealant tape so they would not be covered with resin, Fig. 58.

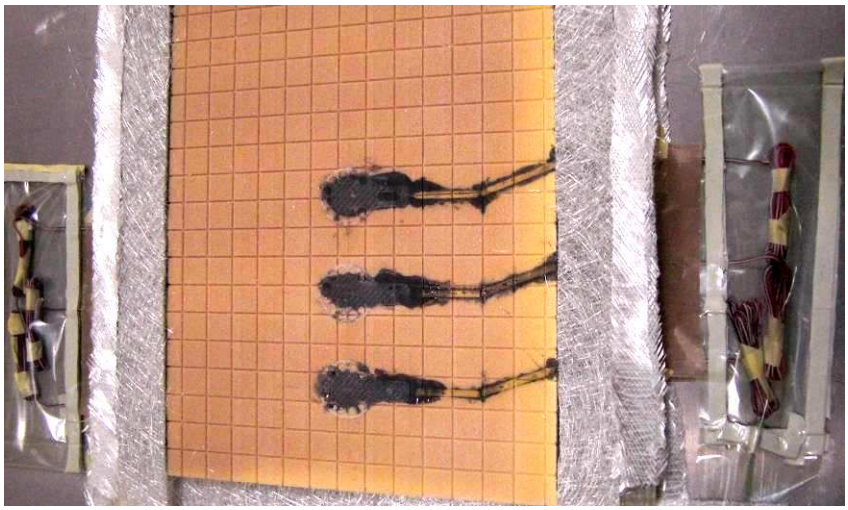


Fig. 58. Lay-up of test specimen with embedded strain gages

Peel ply and a 2mm thick aluminum caul plate were placed over the panel to produce a flat bonding surface for the outer strain gages. The entire specimen was vacuum bagged and infused with Ashland 8084 vinyl ester resin at roughly -90kPa. The infused specimen was cured at room temperature for 24 hours before demolding, then post cured at 70°C for 2 hours. The panel was cut into three dogbone specimens using an abrasive waterjet cutter, Fig. 59. The dogbone shape was loosely based on the ASTM D638 type I standard but scaled to account for the thicker and wider geometry, Fig. 60.

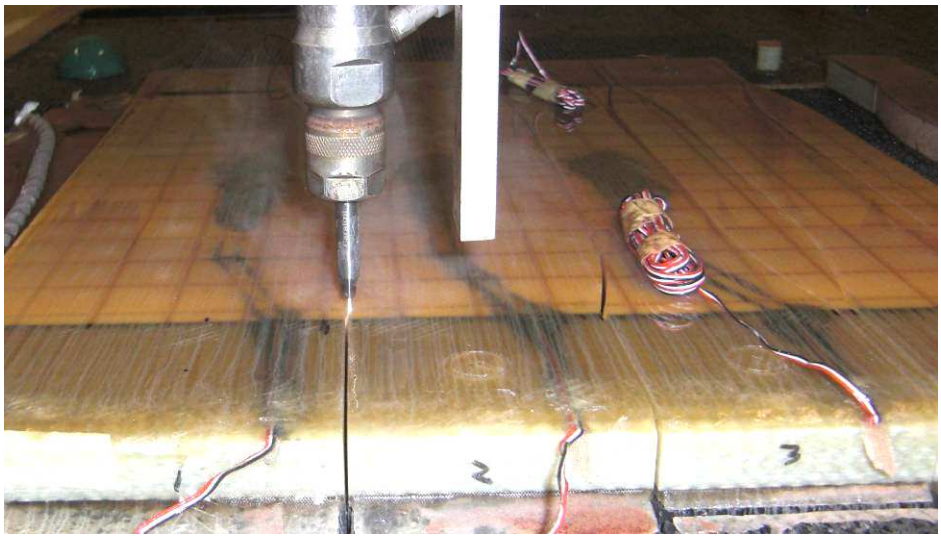


Fig. 59. Waterjet cutting dogbone specimens

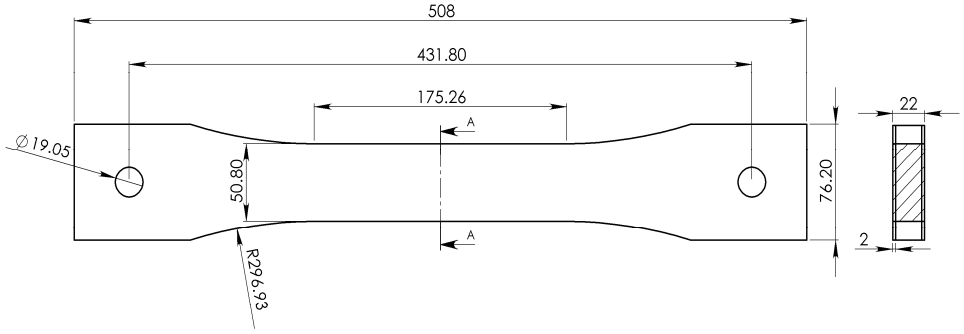


Fig. 60. Dogbone specimen for tensile testing

The pin holes were reamed to 19.05mm diameter, the same size as the attachment pins of the MTI tensile test machine. The strain gages were bonded to the outside of the GFRP skins following Vishay's instruction bulletin [24], Fig. 61.

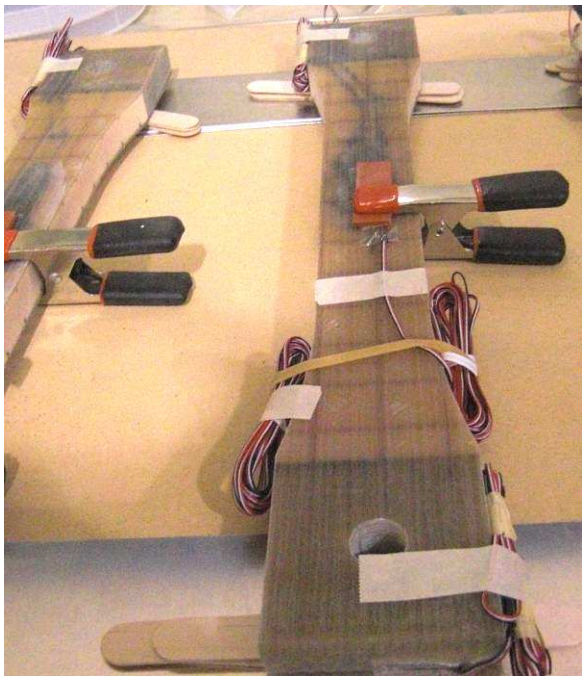


Fig. 61. Bonding strain gages on outer sides of dogbone tensile test specimens.

An aluminum dogbone specimen was also cut on the abrasive waterjet, and strain gages were applied as a reference piece to verify the testing equipment.

Testing

An MTI modified 44kN (10,000 lbs) Instron universal test machine was used for all the tests. The specimens were tested quasi statically under displacement control at 1.5mm/min crosshead velocity. To verify the setup was working properly, the same dogbone profile as the GFRP sandwich was waterjet cut out of 6.5mm thick 6061 T6 aluminum. Strain gages were bonded on both sides in accordance with Vishay's instruction bulletin [24]. The aluminum specimen was loaded and unloaded a number of times and the load and strains were recorded.. The modulus of elasticity was calculated using multiple sets of data and compared with previously tested materials. The modulus was calculated by taking the averages of stresses and strains over several points just after the first unloading, and subtracting them from the averages just before the specimen was fully unloaded. The modulus of the tests recorded by the top and bottom strain gage were 69.8 GPa and 72.2 GPa, respectively, which shows good agreement with previously material test data of 69.0 GPa.

The three GFRP/foam core sandwich dogbone specimens were tested in a similar manner. Data was simultaneously taken from the four strain gages, the load cell, and a displacement transducer. Each specimen was loaded in tension to 5kN, then unloaded to a lower value, and reloaded and unloaded again before proceeding to the next load step 2.5kN higher than the previous. The load increment between each step was 2.5kN and for each step the specimen was loaded and unloaded twice before loading to a new load level. A load verses displacement plot can be seen in fig. 62. This continued until

"pings" were heard from the specimen, around 11.5kN, indicating the onset of localized damage. None of the specimens were tested to complete failure. The maximum strain recorded was 0.85%. The notation used to describe the tests in the next section was specimen number followed by test number, for example, S3T2 would refer to specimen three, second test.

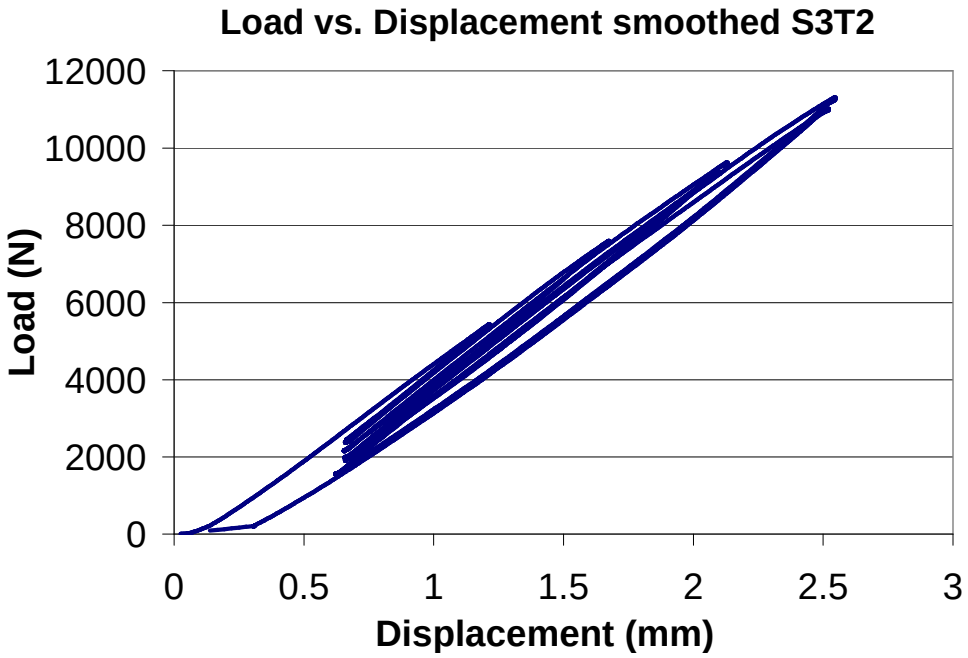


Fig. 62. Load versus displacement for sandwich dogbone tensile specimen.

Summary of results

A typical plot of stress verses strain for the first load step of a sandwich specimen is shown in Fig. 63, displaying all four strain gages; top inner and outer and bottom inner and outer. The "inner" refers to the embedded strain gages and the "outer" to the strain gages bonded on the outside of the GFRP sandwich after it was infused and waterjet cut to shape. The "bottom" refers to the side of the GFRP sandwich which was made in contact with the aluminum table, while the "top" refers to the side of the GFRP sandwich that was in contact with the caul plate during the infusion.

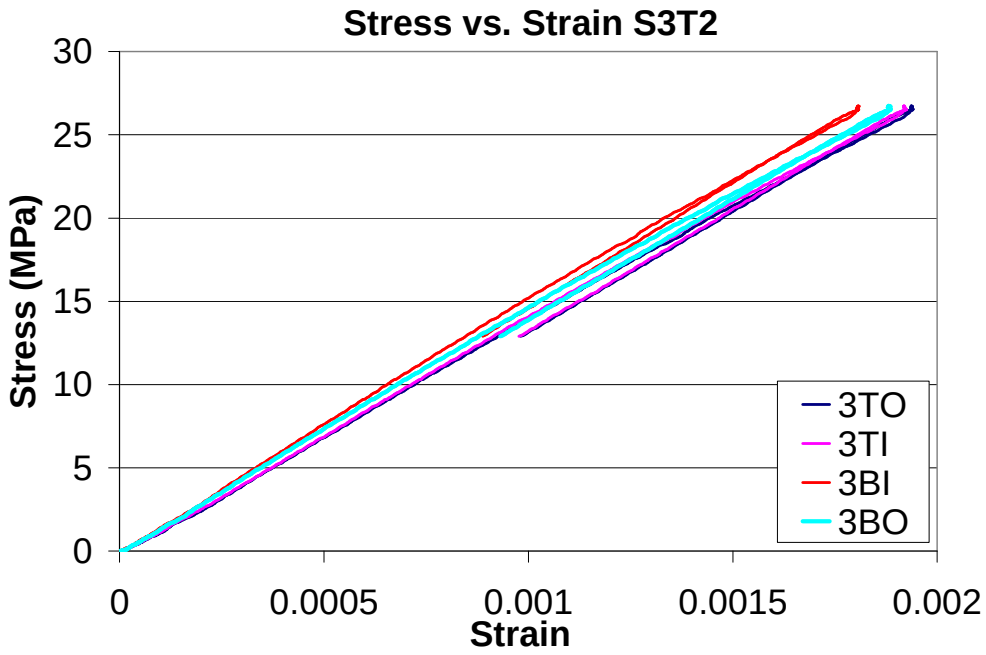


Fig. 63. Stress verses strain for first load step.

The results from the test will be shown in several different ways. The first way is Young's modulus as calculated from the strain from each of the four strain gages. The modulus was calculated by dividing the slope of the load verses strain curve by the cross sectional area of the GFRP skins to get stress over strain for each recorded strain gage. The slope was calculated using the average stress and strain of several data points right after the first loading and subtracting them from several data points right before the specimen was fully unloaded, . The resulting four Young's moduli were then averaged. A comparison between the different specimens and different tests can be seen in Fig. 64. The figure shows good agreement between the three different specimens, as well as the third specimen loaded three different times. The modulus of the third specimen appears to decrease during subsequent tests which could be caused for example by microcracking in the matrix during loading. Some scatter might be expected for multiple reasons, including inhomogeneity of the fiberglass, the fiberglass layers could be orientated slightly different, the strain gages may be mounted slightly off axis, etc.

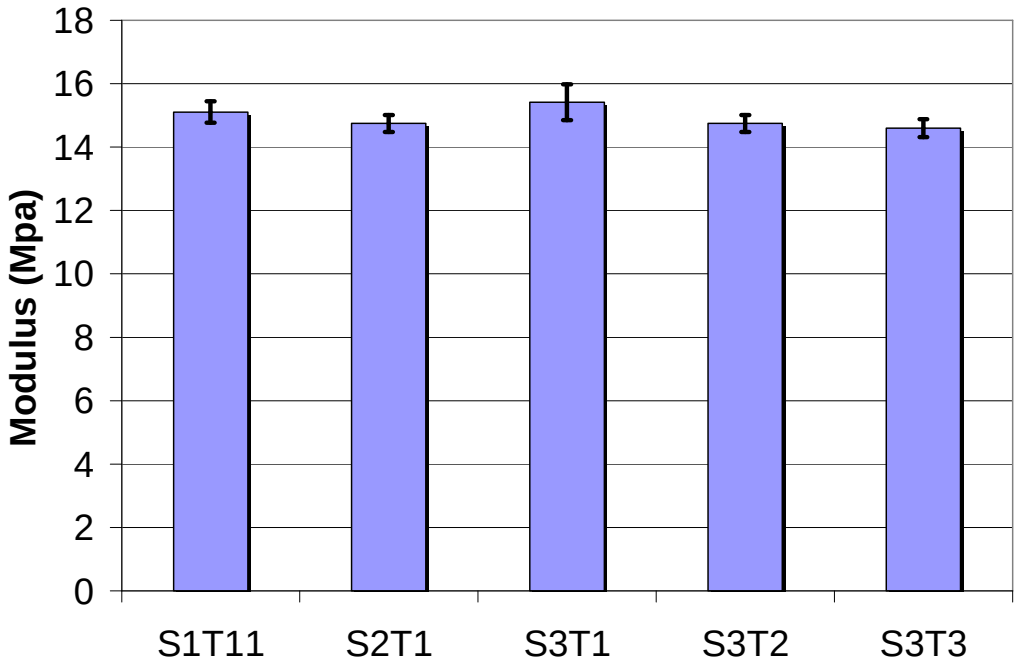


Fig. 64. Young's modulus of the sandwich skins. The modulus was calculated from all four strain gages. The error bars indicated standard deviations resulting from the four different strain gages.

Typical strain gage values were taken at different strain levels and the difference was calculated between the inner (embedded) and the outer strain gages for both top and bottom pairs. The result is shown in Table 9. The top mounted strain gages appear to strain more, indicating that there may be some bending during the test. The embedded inner strain gages show good correlation with the outer strain gages and are within 3% relative difference of each other.

Table 9. Typical strain gage values and their percent difference.

Load	Displ.	Strain (%)				% Difference	
(N)	(mm)	2TO	2TI	2BI	2BO	Top	Bottom
4811	1.2	0.200	0.199	0.188	0.192	0.31	-2.31
7578	1.7	0.299	0.296	0.283	0.291	1.01	-2.60
10991	3.6	0.601	0.617	0.588	0.593	-2.61	-0.86
13560	4.1	0.699	0.708	0.684	0.693	-1.20	-1.24

Chapter 5

Summary, Conclusions, and Recommendations for Future Work

In chapter two, doubly curved sandwich panels were studied numerically and experimentally. The numerical analyses confirmed that there may be substantial benefits in using curved sandwich panels, but that not all curved panels are superior to flat counterparts. Molds were efficiently made by CNC routing low cost foam. Curved sandwich panels were made by covering the foam molds with a thin film and vacuum infusing the panels directly in these foam molds. Test panels were adhesively bonded to a steel fixture and tested under hydrostatic water pressure.

Several conclusions were drawn from the work done in chapter two. Doubly curved composite sandwich panels with a thin light foam core and stiff skins in comparison to a flat panel is much more affected by an increase in curvature than a panel with a thick, denser foam core and less stiff skins. A time and cost effective method for fabricating a doubly curved panel is to first CNC route the shape from a high density foam, then CNC route the foam core flat and thermoform it to shape in the mold, then cover the mold with either epoxy or vacuum bag and layup the panel and vacuum infuse. For the panel to be watertight care must be taken during vacuum infusion so there are no air leaks. A combination of solid and shell elements modeling the composite sandwich panel and steel test collar is recommended for predicted results to be reasonable to experimental. The predicted stiffness results showed good correlation to experimental results, within 1.2% difference for deflection, whereas the strength predictions showed

some discrepancy. The discrepancy is believed to be mainly due to using a very simple wrinkling formula.

Future work should include refined strength predictions to improve the predicted values and account for the waviness of a woven face sheet including experimental validation. It would be beneficial to experimentally test the phenomenon of shallowly curved panels deflecting less than flat sandwich panels as the reason for this is not fully understood. The methods for forming foam cores for relatively small panels worked well but probably won't work on a larger panel. It would be useful for the development of different methods for forming foam cores, specifically, methods applicable to much larger sheets of foam.

Previous work has been done on a 1:35 scale hybrid hull concept of a destroyer class ship having a steel frame designed to take the global bending loads, and bonded fiberglass sandwich panels designed to take shear and water pressure loads.
In chapter three, work has been extended to build a much larger 1:8 scale hybrid hull concept of a destroyer class ship and study its fatigue performance. Flat and corrugated composite sandwich panels were designed, analyzed and manufactured to be tested under cyclic testing. Tests were done to determine the surface preparation, bonding area, and bond material. A fixture was built to hold the panels while epoxy was applied and then clamp the panels to the steel frame while the epoxy cured.

Several conclusions were drawn from the work done in chapter three. For this application, flat composite sandwich panels can replace steel sections and weigh 87% less. The weight can be further reduced to 90% lighter than steel by making the composite sandwich panels corrugated. Composite sandwich panels were designed with a 1.54mx1.29mx44mm foam core having a 125mm corner radius, 45 degree taper, and 100mm blending radius. The single skin edge should be 125mm giving the panel 25mm an unsupported single skin fiberglass edge with a 100mm bonding overlap. When fabricating large flat and corrugated panels smaller pieces of foam core should be bonded together and routed to final shape then layed up for vacuum infusion. To bond the foam core pieces together hourglass shaped keys work well to align the pieces of foam core and hold them in place while the epoxy cured. When laying up corrugated panels, the fibers, resin distribution medium, peel ply, and vacuum bag should be laid in place and held down with a block conforming to the core, then vacuum bagged. For panel bonding it is important to carefully prepare the two surfaces for bonding. The steel of the beam was sanded with a 40 grit grinding wheel, and cleaned with trichloroethylene. Dow Silane 6011 was wiped onto the beam one hour prior to bonding. Henkel E2119 epoxy adhesive was used for bonding with approximately 0.1% by volume 0.18mm max diameter glass beads to control bond thickness. In order to clamp the panel together to allow the epoxy to cure an aluminum bonding fixture was built to hold the panel temporarily in place with vacuum suction cups then ratchet-strapped to the steel beam. A three point bending fatigue testing fixture was developed, and the specimen was successfully fatigue tested for 325,000 cycles. Cracks were

found in the steel of the specimen, but almost no damage occurred in the bonded joints or the composite panels.

Future work should include testing the steel/composite hybrid hull concept in sea trials. Simplified testing of the hybrid hull concept has been very promising but there might be unforeseen behavior when the hybrid hull is subjected to a combined dynamic loading. Specifically, the stiffness mismatch of the relatively compliant single skin composite and the relatively stiff steel frame could pose problems for the structural and watertight integrity of the hull in a dynamic loading.

In chapter four, a method for embedding strain gages inside a composite sandwich panel was successfully developed and tested. A panel was manufactured with strain gages bonded to a thin GFRP paddle which was bonded to a foam core. The strain gage wires were routed through the foam core near neutral axis of the sandwich panel, and out through the inner GFRP skin and reinforcement layers. The panel was then vacuum infused. The procedure was very successful, resulting in good quality panels and free strong electric wires exciting nicely from the inside. A second panel was manufactured to test the accuracy of the embedded strain gages. The panel was waterjet cut into dogbone specimens and strain gages were attached to the outside of the panel as well before being tested in tension. The strain gages' measured values were within 3% of each other, suggesting that this method of measuring strain is within acceptable accuracy for the intended marine application.

Future work should include additional testing of the embedded strain gages while varying the temperature. The embedded strain gages could react differently to changes in temperature compared to strain gages attached on the outside of a panel. It would be useful to develop different methods for embedding strain gages to make this concept more robust for different applications.

References

1. Librescu, L., Hause, T., “Recent developments in the modeling and behavior of advanced sandwich constructions: a survey,” Composite Structures, 48, 2000, pp. 1-17.

2. Hohe, J., Librescu, L., “A nonlinear theory for doubly curved anisotropic sandwich shells with transversely compressible core,” International Journal of Solids and Structures 40. 2003. pp. 1059-1088.

3. Drake, K. R., Neo, S. C., Blackie, A. P., “Approximate analysis of a square flat top sandwich panel with a curved bottom skin,” Composite Structures 7. 2006. pp. 354-360

4. Burton, W., Noor, A., “Assessment of computational models for sandwich panels and shells,” Computer methods in applied mechanics and engineering. 124. 1995. pp. 125-151.

5. Skvortsoc, V., Bozhevolnaya, E., Kildegaard, A., “Assessment of models for analysis of singly curved sandwich panels,” Composite Structures 41. 1998. pp. 289-301.

6. O'Sullivan, D., Slocum, A., "Design of two-dimensionally curved panels for sandwich cores," Journal of Sandwich Structures and Materials, 5. 2003. pp.77-97.

7. Russo, A., Zuccarello, B., "Experimental and numerical evaluation of the mechanical behavior of GFRP sandwich panels," Composite Structures 81. 2007. pp. 575-586.

8. MacDonald, D., Chen, Y., "Mechanical analysis of simply supported curved rectangular sandwich panels subjected to general loading," Fibre Science and Technology. 10. 1977. pp. 65-85.

9. Thompson, L., Walls, J., Caccese, V., "Design and analysis of a hybrid composite/metal structural system for underwater lifting bodies," Project Report for the Modular Advanced Composite Hull form (MACH) Technology Project. Report No. UM-MACH-RPT-01-08. 2005.

10. Cunningham, P. R., White, R. G., Aglietti, G. S., "The Effects of Various Design Parameters on the Free Vibration of Doubly Curved Composite Sandwich Panels," Journal of Sound and Vibration, Vol. 230, Issue 3, Feb. 2000, pp. 617-648

11. Kuppusamy, A., “Development of framework for rapid tool manufacture for RIDFT process,” (MS Thesis, Florida State University, 2003).

12. McCaffery, T., Zguris, Z., Durant, Y., “Low cost mold development for prototype parts produced by vacuum assisted resin transfer molding (VARTM),” Journal of Composite Materials, 37. 2003. pp. 899-912.

13. Cao, J., Grenestedt, J.L., Maroun, W.J., "Testing and analysis of a 6-m steel truss/composite skin hybrid ship hull model," Marine Structures, Vol. 19, 2006, pp. 23-32.

14. Cao, J., Grenestedt, J.L., Maroun, W.J., “Steel Truss/Composite Skin Hybrid Ship Hull, Part I: Design and Analysis,” Composites Part A, Volume 38, 2007, 1755-1762.

15. Maroun W., Cao, J., Grenestedt, J.L., “Steel truss/composite skin hybrid ship hull. Part II: Manufacturing and sagging testing,” Composites Part A, Volume 38, 2007, 1763-1772.

16. Grenestedt, J.L., Cao, J., Maroun, W.J., "Test of Extensively Damaged Hybrid Ship Hull," Journal of Marine Science and Technology, Vol. 13, No. 1, 2008, pp. 63-70.

17. Ansys 9.0 Technical Manual

18. Hoff, N.J., Mautner, S.E. The Buckling of Sandwich-Type Panels. J. Aero. Sci., Vol. 12, 1945, pp. 285-297, eq. (103).

19 DIAB. Divinycell H-Grade Technical Manual, 10.00. DIAB AB, Laholm, Sweden

20. Indirect Personal correspondence with Chris Kilburn.

21. Thermoforming Technical Bulletin, Diab website.

22. Owens Corning. Kyntex Woven Rovings Technical Data Sheet. One Owens Corning Parkway, Toledo, OH 43659

23. Ashland Derakane. Technical Data Sheet for Derakane 8084 Resin. Columbus, OH

24. Vishay Instruction Bulletin B-137-Strain Gage Applictions with M-Bond AE-10, AE-15 and GA-2 Adhesive System, Revision 4/05, Document No. 11137.

25. Melograna, J.D., Grenestedt, J.L., "Adhesion of Stainless Steel to Fiber Reinforced Vinyl Ester Composite," Journal of Composites Technology and Research, Vol. 24, No. 4, 2002, pp. 254-260.

26. Sovereign Specialty Chemicals SIA E2119 A/B Technical Data Sheet.

27. Grenestedt, J.,L., Bassinet, F., “Influence of Cell Wall Thickness Variations on Elastic Stiffness of Closed-Cell Cellular Solids,” International journal of Mechanical Sciences, Volume 42, 2000, 1327-1338.

28. Barsoum R. “The best of both worlds: hybrid ship hulls use composites and steel,” AMPTIAC Quarterly 2003; 7(3):55-61

29. Barsoum R. Hybrid ship hull. US Patent 6, 386 1313; 14 May, 2002.

30. Cao J., Grenestedt J.L. “Design and testing of joints for composite sandwich/steel hybrid ship hulls,” Composites Part A 35; 2004; 1091-1105.

31. Reany, J, and Grenestedt, J.L. “Corrugated Skin in a Foam Core Sandwhich”, Composite Structures, available online October 2008.

32. Yen, B., Huang, T., Lai, L., Fisher, J., “Manual for Inspecting Bridges for Fatigue Damage Conditions,” Department of Civil Engineering Report No. 511-1, Lehigh University, Bethlehem PA, January 1990.

33. Shunkla, A., Practical Fracture Mechanics in Design, New York, CRC, 2004

34. Guemes, J., Menedez, J., “Response of Bragg grating fiber-optic sensors when embedded in composite laminates,” Composites Science and Technology, Vol. 62, June 2002, pp. 959-966.

35. Grenestedt, J., Reany, J., “Design of Steel / Composite Hull for Slamming Load Test Facility,” in preparation.

Appendix A

Figures A1-A5 show the ANSYS models of the double curved panels. All figures show models with the thickness feature turned on which is a graphical representation of the thickness of the shell elements. The core modeled with solid elements with the skins as shell elements is shown in Fig. A1. The sandwich panel modeled using shell elements with the tapered section highlighted where it is modeled with and without the sandwich option turned on is shown in Fig. A2. Figures A3-A5 show the model with shell elements with no taper, with a taper, and with a taper with the fixture modeled, respectively.

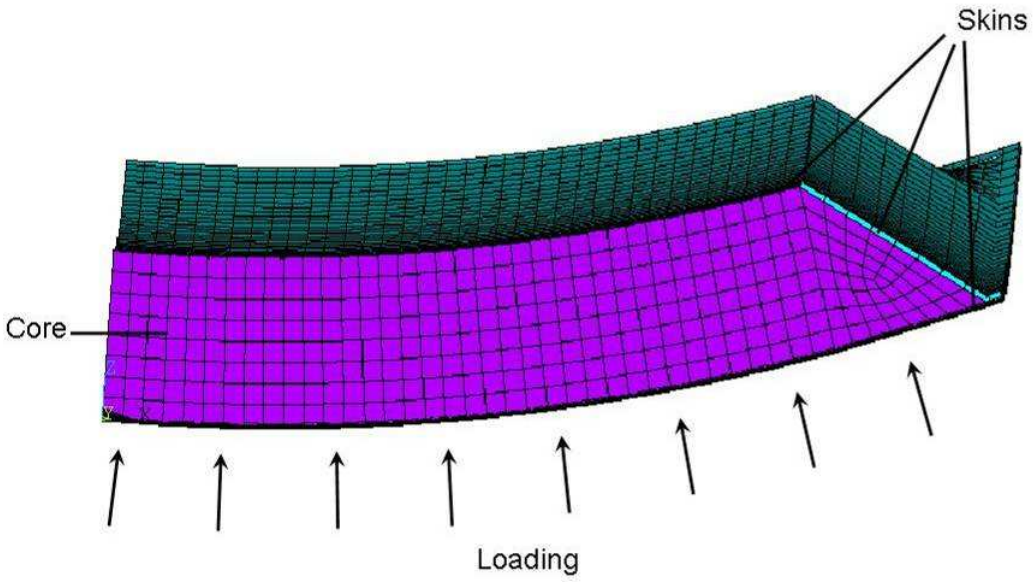


Fig. A1. Solid and shell elements.

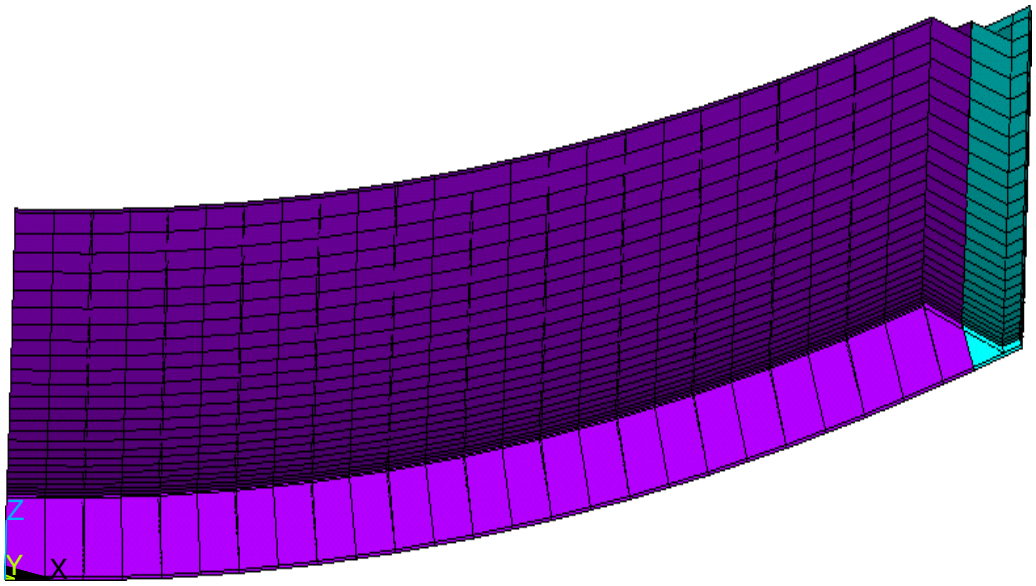


Fig. A2. Shell elements with the sandwich option turned off in green and turned on in purple.

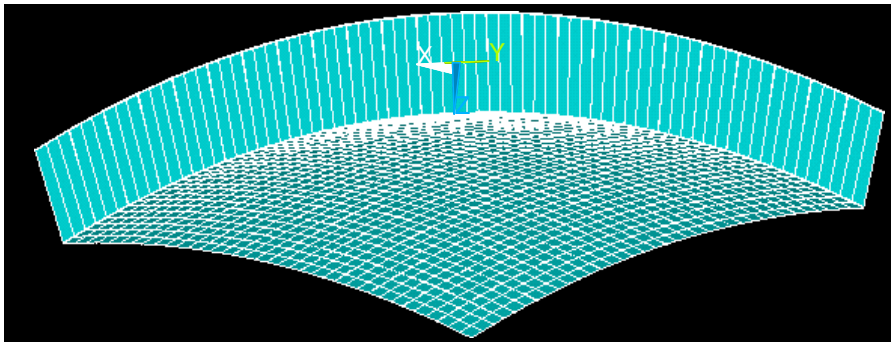


Fig. A3. Shell elements with no taper.

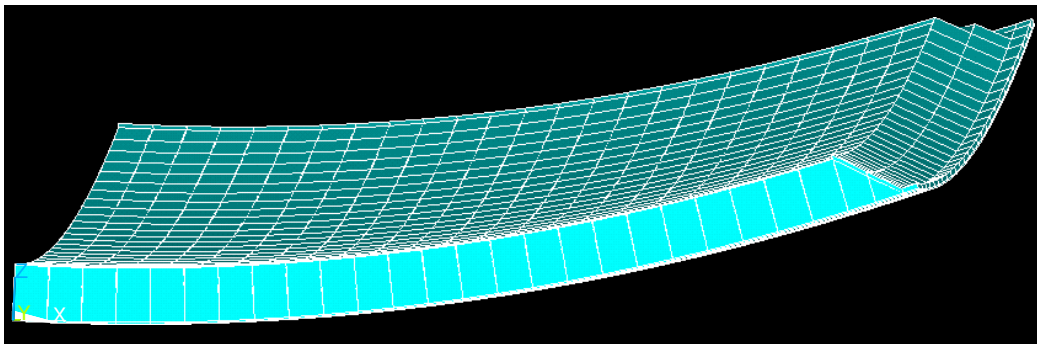


Fig. A4. Shell elements with taper.

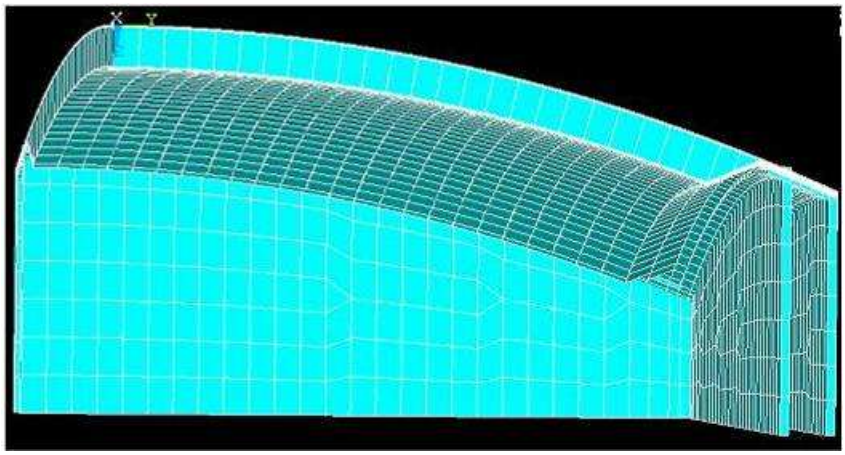


Fig. A5. Shell elements with tape and fixture modeled.

Vita

Andrew Truxel was born on April 29, 1981 in Somerset, New Jersey to his parents, George and Martha. He resided in Warren, NJ where he attended Warren Middle School and Watchung Hills Regional High School. He received three varsity letters in football and four varsity letters in wrestling. In August of 1999 he began his studies at Lehigh University. During his undergraduate studies he was inducted into Phi Eta Sigma and Pi Tau Sigma honor societies. He graduated in May 2003 with a BS in Mechanical Engineering and a minor in Economics. He continued his studies at Lehigh University for his Masters of Science followed by his PhD in Mechanical Engineering while working as a research assistant in the Lehigh Composites Lab headed by Dr. Joachim L. Grenestedt.